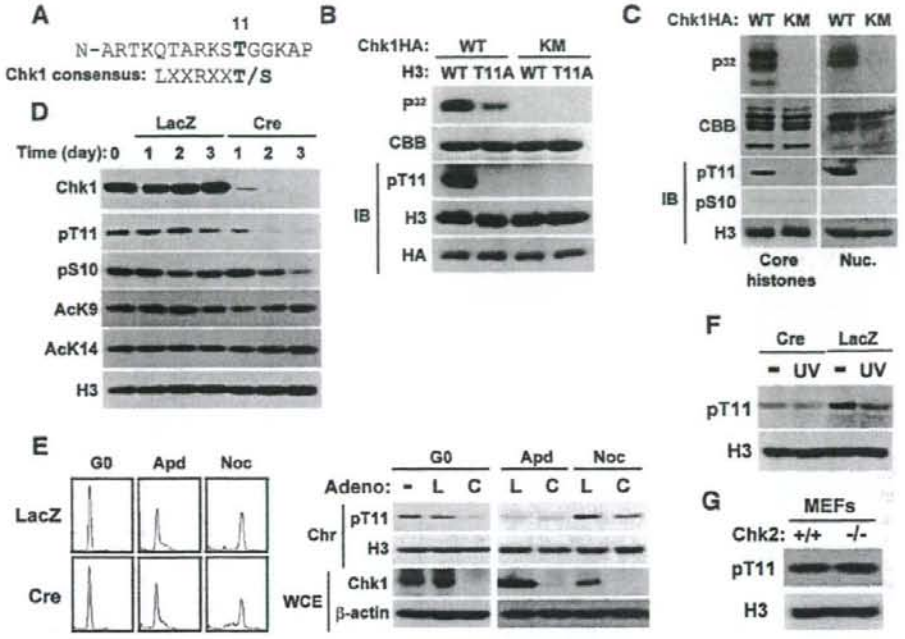

Figure 3. Chk1 Phosphorylates Histone H3-T11 Both In Vitro and In Vivo

(A) Alignment of the H3 N-terminal tail and the Chk1 phosphorylation consensus motif. The residues of H3 presented in bold fit the minimum consensus motif.

(B) Immunopurified Chk1-HA (WT) and Chk1-K38M-HA kinase-deficient mutant (KM) were used for in vitro kinase assays on purified wild-type H3 (WT) or H3-T11A (T11 substituted with A) as substrate. Top two panels: products were separated by SDS-PAGE (15%) and visualized by autoradiography (P^{32}) and Coomassie-brilliant blue (CBB). Bottom three panels: a reaction without P^{32}ATP was subjected to immunoblotting using the indicated antibodies to phospho-T11 (pT11) or H3 (H3). Immunoprecipitated Chk1-HA (WT) and Chk1-KM-HA (KM) were detected using anti-HA antibodies.

(C) Chk1 kinase assay was performed as in (B) using core histones (core histones) or nucleosomes (nuc) as a substrate. Top two panels: results of autoradiography (P^{32}) and CBB staining (CBB). Bottom three panels: the reaction without P^{32}ATP subjected to immunoblotting using the indicated antibodies.

(D) Chk1$^{flox/-}$ MEF cells were infected with either Ade-LacZ (LacZ) or Ade-Cre (Cre) and harvested at the indicated times after infection. Chromatin fractions were prepared and analyzed by immunoblotting using the indicated antibodies.

(E) (G0) Chk1$^{flox/-}$ MEFs were rendered quiescent by serum starvation and infected with Ade-LacZ (L) or Ade-Cre (C). Cells were cultured for an additional 2 days under serum-starved condition. Chk1$^{flox/-}$ MEFs were infected with Ade-LacZ or Ade-Cre and cultured in medium containing aphidicolin (Apd) for 2.5 days. Chk1$^{flox/-}$ MEFs were infected with Ade-LacZ or Ade-Cre and cultured in medium containing nocodazole (Noc) for 2.5 days. Cell-cycle distributions were determined by FACS analysis (left), H3-T11 phosphorylation status and H3 were analyzed by immunoblotting using chromatin fractions (Chr), and Chk1 and β-actin were done using whole-cell extracts (WCE) (right).

(F) Chk1$^{flox/-}$ MEFs were infected with Ade-LacZ (LacZ) or Ade-Cre (Cre), irradiated with UV 2 days after infection and harvested 4 hr after irradiation. Chromatin fractions were prepared and H3-T11 phosphorylation status analyzed by immunoblotting.

(G) H3-T11 phosphorylation was analyzed as in (D) using wild-type or Chk2$^{-/-}$ MEFs.

inhibitor of the ATM and ATR kinases, inhibited Chk1 release from chromatin and maintained H3-T11 phosphorylation in response to DNA damage (Figure 4B). We also observe that caffeine prevents the DNA damage-dependent loss of *cdk1* and *cyclin B1* transcripts. Thus, the reduction of H3-T11 phosphorylation is PIKK dependent and correlates with Chk1 chromatin dissociation and with the transcriptional status of *cdk1* and *cyclin B1*.

UV-induced Chk1 phosphorylation is dependent on ATR but not ATM (Brown and Baltimore, 2003), and UV-induced Chk1 dissociation requires ATR (Smits et al., 2006). ATR-specific but not control siRNA significantly reduced ATR protein level, UV-induced Chk1 dissociation, and H3-pT11 dephosphorylation (Figure 4C). UV-induced Chk1 chromatin dissociation is known to require ATR-dependent phosphorylation at Chk1-S317 and -S345. A Chk1-S317A/S345A mutant (Chk1-SA) is retained on chromatin in the presence of DNA damage (Nilda et al., 2007; Smits et al., 2006). HCT116 cells expressing Chk1-SA-myc, but not cells expressing Chk1-myc, retained significant Chk1-SA-myc on chromatin following UV treatment (Figure 4D). Furthermore, H3-T11 phosphorylation and *cyclin B1* plus *cdk1* expression were partially restored only in cells expressing Chk1-SA-myc. These results confirm that H3-T11 dephosphorylation and suppression of *cyclin B1* plus *cdk1* expression are dependent on the Chk1 chromatin dissociation.

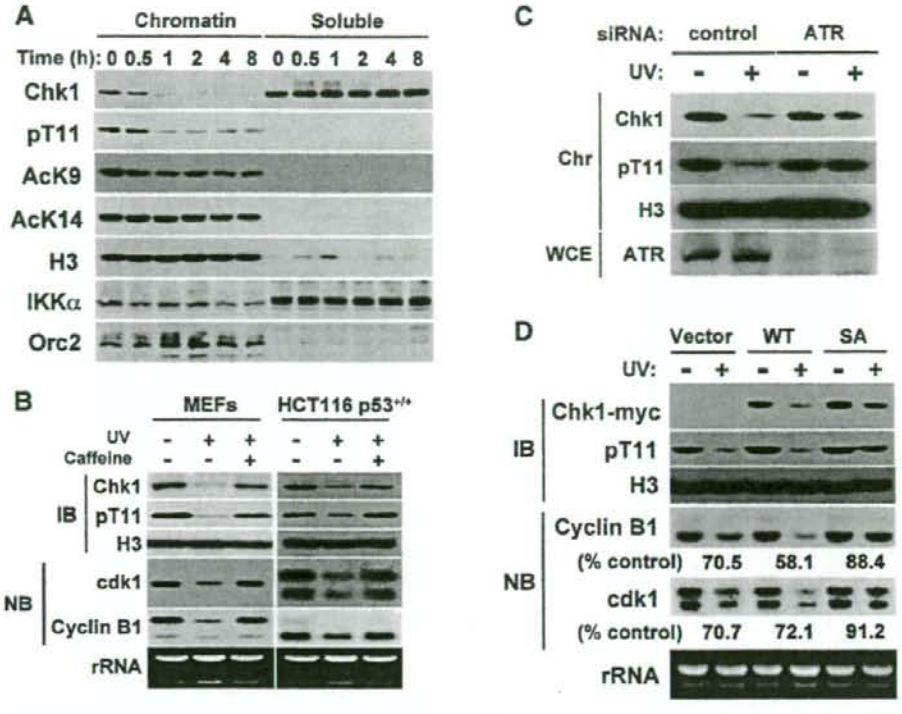

Figure 4. Release of Chk1 from Chromatin following DNA Damage Correlates with Decreased H3-T11 Phosphorylation

(A) Chk1$^{flox/-}$ MEF cells were exposed to UV irradiation (500 J/m^2) and harvested at the indicated times, and chromatin fractions and soluble material were prepared for analysis by immunoblotting with the indicated antibodies.

(B) Chk1$^{flox/-}$ MEFs or HCT116 p53$^{+/+}$ cells were preincubated in the presence (+) or absence (–) of 20 mM caffeine for 10 min and either exposed or not to UV irradiation (500 J/m^2). Cells were harvested after 2 hr, chromatin fractions were prepared and immunoblotted as described in (A), or RNA levels examined by northern blot analysis with the indicated probes. rRNA is shown as a control.

(C) HCT116 p53$^{+/+}$ cells were transfected with control or ATR siRNA. After 72 hr, cells were treated with (+) or without (–) UV (180 J/m^2). After 1 hr incubation, cells were harvested and immunoblotting analysis was performed on chromatin fractions for Chk1, H3-pT11, and H3 and on whole-cell extract for ATR.

(D) HCT116 p53$^{+/+}$ cells were transfected with empty vector or expression vector encoding Chk1 wild-type (WT) or Chk1-S317A/S345A (SA) protein. After 48 hr, the cells were treated with (+) or without (–) UV (250 J/m^2). Chromatin fractions were prepared for immunoblot analysis after 1 hr incubation or RNA was extracted after 4 hr incubation. Northern blot analysis was performed with the indicated probes as described above. Intensity is presented as a % of –UVcontrol.

Transcriptional Reduction of Cell-Cycle Regulators after Chk1 Depletion in Somatic Cells

To test whether Chk1 depletion should result in transcriptional repression of the same genes repressed in response to DNA damage, we assayed the consequences of Chk1 depletion in MEFs. Three days after Chk1 depletion by Ade-Cre virus transfection, Chk1$^{-/-}$ MEFs did not undergo premature mitosis but arrested in S phase (Figure 5A). Loss of the inhibitory Y15 phosphorylation of cdk1 occurred after 2 days in our Chk1$^{-/-}$ MEFs, in much the same way as has been reported for ES cells. However, cyclin B1 protein was significantly reduced (Figure 5B) and at 3 days both cdk1 and cyclin B1 protein levels were very low. This presumably explains why Chk1-depleted MEFs do not prematurely enter mitosis. Important for our work, the reduction in cyclin B1 and cdk1 proteins correlates with decreased levels of the corresponding mRNA (Figure 5C). The steady-state levels of *PCNA*, *DHFR*, and *KCNK1* mRNA were not significantly affected by Chk1 depletion. Thus, after DNA damage or Chk1 depletion in MEFs, *cdk1* and *cyclin B1* (but not other E2F-target genes such as *PCNA* and *DHFR*) are transcriptionally repressed. This indicates that Chk1 is required for the correct expression of *cyclin B1* and *cdk1*.

Although Chk1-SA-myc does not restore cell-cycle checkpoint functions (Nilda et al., 2007), it did partly suppress the cell-cycle arrest defect (Figure 5D), prevent H3-T11 dephosphorylation, and partially stabilize *cyclin B1* plus *cdk1* expression (Figure 5E). Interestingly, unlike expression of wild-type Chk1-myc, Chk1-SA-myc failed to prevent DNA damage-dependent γ-H2AX accumulation as a consequence of the endogenous Chk1 depletion, presumably because it is compromised for checkpoint functions. Thus, Chk1-SA-myc, which is not released

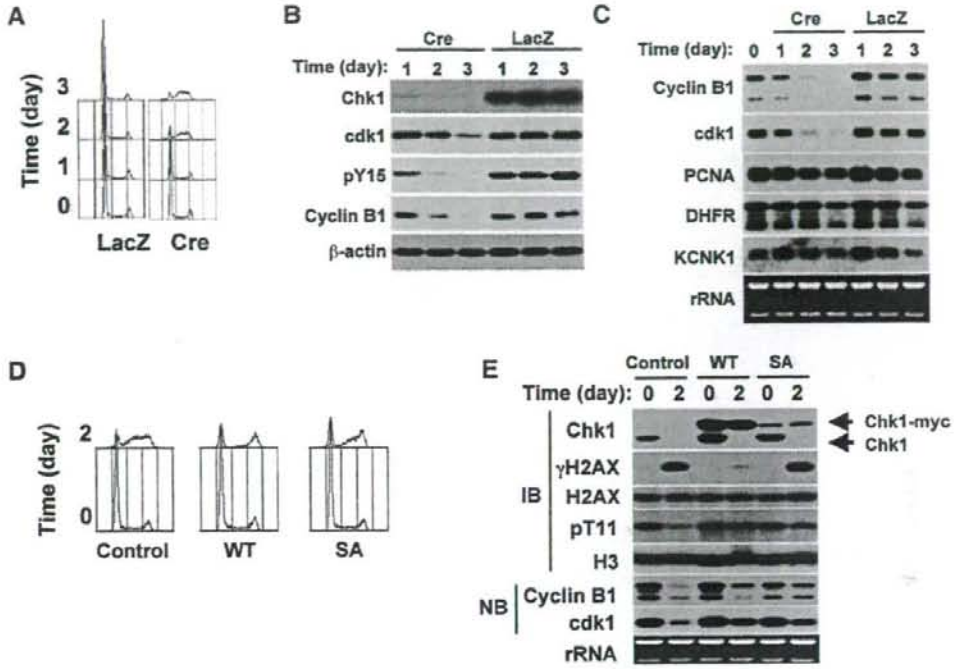

Figure 5. Chk1 Depletion in MEFs Results in S Phase Arrest But Not Mitotic Catastrophe

$Chk1^{flox/-}$ MEFs were infected with Ade-LacZ or Ade-Cre and harvested at the indicated days after infection. (A) Cell-cycle distribution was determined by FACS analysis. (B) Soluble extracts were prepared and subjected to immunoblotting with the antibodies indicated. (C) Northern blot analysis used the probes indicated. (D) $Chk1^{flox/-}$ MEFs expressing Chk1 wild-type (WT) or Chk1-S317A/S345A (SA) were infected with Ade-Cre. After 2 days of infection, the cells were prepared for FACS analysis. (E) Chromatin was analyzed by immunoblot and RNA was analyzed by northern blotting.

from chromatin after DNA damage, results in maintenance of H3-T11 phosphorylation and expression of *cyclin B1* plus *cdk1* in the presence of DNA damage.

To establish the extent of Chk1-dependent transcriptional maintenance, we conducted microarray experiments to investigate the global requirement for Chk1 in gene expression. Cells rendered quiescent by serum starvation were infected with Ade-Cre or the control Ade-LacZ viruses and held for 2 days, and mRNA were prepared and analyzed by hybridization to microarrays (Filgen Array mouse 32K, oligo DNA microarray). We observed that 214 transcripts were downregulated following Chk1 depletion (Table S1). Thus, Chk1 is required for the correct expression of many genes in vivo. We chose three genes, *pctk2*, *trib2*, and *HMGA2* and confirmed that their expression was repressed in response to DNA damage, further linking the function of Chk1 to DNA-damage-induced transcriptional repression.

GCN5 HAT Preferentially Binds to Phosphorylated H3 Peptide In Vitro

Computer modeling suggested that H3-T11 phosphorylation could enhance binding of the GCN5 HAT to nucleosomes (Figure S3). We therefore examined whether H3-T11 phosphorylation influences the ability of GCN5 to bind to an H3 tail peptide. Four synthetic H3 peptides, S10/T11, pS10/T11, S10/pT11, and pS10/pT11, differing only by the presence or absence of a phosphate group at the S10 and T11 residues were used as substrates in SPR Biosensor Binding Analysis with yeast GCN5 (aa 100–255) purified from insect cells (Figure 6).

In the presence of CoA (0.15 mM), GCN5 bound to H3-pT11, H3-pS10, and H3-pS10/pT11 with similar dissociation constants (Figure 6C). Binding to unphosphorylated H3 peptide showed ~20-fold lower affinity. Intriguingly, in the absence of CoA, binding affinities between GCN5 and two peptides were significantly reduced. CoA-dependent binding of GCN5 to the H3 peptide was predicted by structural analysis of GCN5/CoA/histone ternary complex, in which CoA is required to reorient the enzyme for histone binding (Rojas et al., 1999). Our results show that either H3-T11 or H3-S10 phosphorylation dramatically enhances the preference of GCN5 for H3.

H3-T11 Phosphorylation Is Involved in Recruitment of GCN5 at the Sites of *cdk1* and the *cyclin B1* Promoter

As we see a modest decrease in H3-K9 acetylation, an attractive model is that H3-T11 phosphorylation by Chk1 results in GCN5

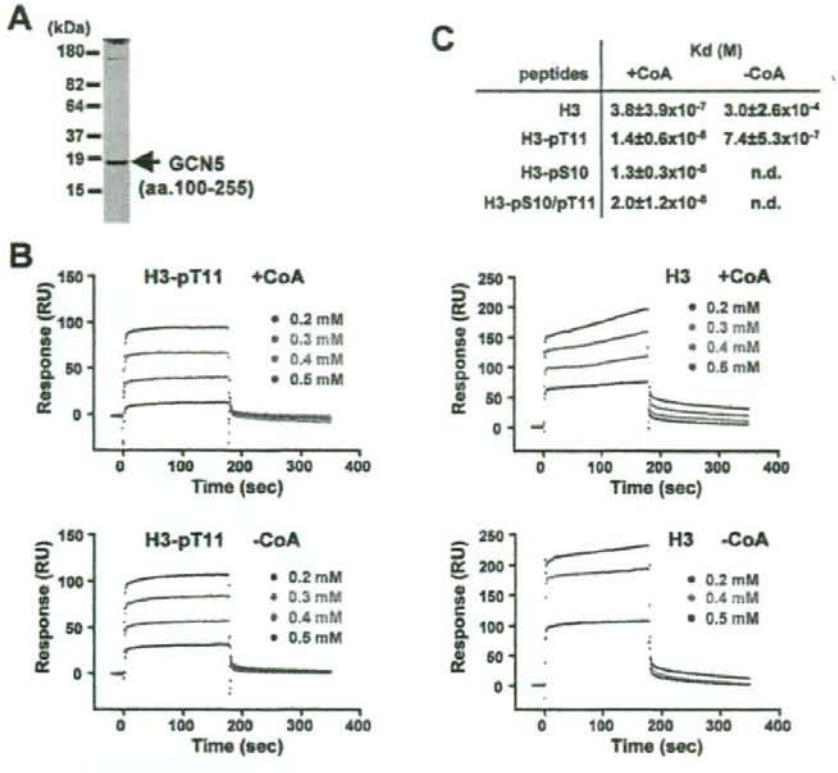

Figure 6. GCN5 Has Increased Affinity for H3-pT11 Peptide

(A) CBB staining of purified yeast GCN5 HAT domain (aa 100–255).

(B) BIAcore analysis of the interaction between GCN5 and H3 peptides. The purified GCN5 from (A) was immobilized on the surface of biosensor Chips.

(C) Binding affinities (Kd [M]) between GCN5 HAT and H3 peptides. Data were collected in the presence or absence of CoA. Values from three independent experiments are shown as means ± SD.

recruitment and transcriptional activation via lysine acetylation. To explore the possibility that GCN5 is mechanistically involved in Chk1-dependent transcriptional repression following DNA damage, we used chromatin immunoprecipitation (ChIP) to test for the presence of H3-T11 phosphorylation, H3-K9 and -K14 acetylation, and Chk1 and GCN5 proteins at the promoters of *cdk1* and *cyclin B1* (transcriptionally repressed following DNA damage) and at the promoter region of *GAPDH* (transcription unaffected by DNA damage).

We established that Chk1 was present at all three promoter regions in unperturbed cells. Following DNA damage (Figure 7A) or Chk1 depletion (Figure 7B) by Ade-Cre infection, Chk1 was barely detectable at any of the three promoter regions. As predicted, the level of H3-T11 phosphorylation was concomitantly reduced at all promoters following both treatments. Neither Chk1 nor H3-T11 phosphorylation was observed at subtelomeric regions or in the intergenic regions upstream or downstream of *cyclin B1* (Figure 7C). Because H3-T11 phosphorylation was particularly enriched at centromeres during mitosis (Preuss et al., 2003), H3-T11 phosphorylation, but not Chk1, was detected at the centromeric region. Of particular interest, we found that H3-K9 acetylation strongly correlated with H3-T11 phosphorylation on the promoter regions of both *cdk1* and *cyclin B1* but did not correlate with H3-T11 phosphorylation at the *GAPDH* promoter region. *GAPDH* transcription is not repressed by either DNA damage or Chk1 depletion and thus does not correlate with Chk1 status. We observed that GCN5 was present at the promoter regions of *cdk1* and *cyclin B1* in unperturbed cells but was not detected at the promoter region of *GAPDH*. Furthermore, GCN5 levels at *cdk1* and *cyclin B1* promoters were significantly reduced in response to either DNA damage or Chk1 depletion. These results are consistent with a model whereby Chk1-mediated transcriptional repression is mediated by the loss of GCN5 recruitment to promoter regions of target genes when Chk1 dissociates from the chromatin and H3-T11 becomes dephosphorylated. The subsequent reduction in acetylation of K9 presumably reflects the associated change in promoter-bound HAT activities.

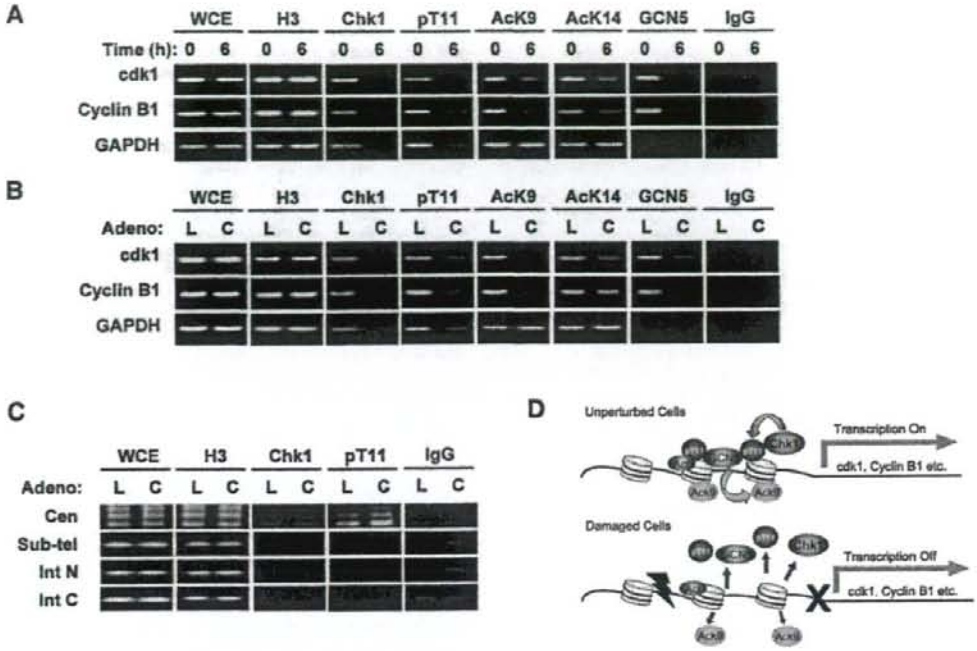

Figure 7. DNA Damage or Chk1 Depletion Results in Decreased H3-T11 Phosphorylation and Decreased H3-K9 Acetylation, which Correlates with GCN5 Recruitment to *cdk1* and *cyclin B1* Promoters

(A) Chk1$^{flox/-}$ MEF cells were left untreated or exposed to UV irradiation.

(B and C) The Chk1$^{flox/-}$ MEFs were infected with Ade-LacZ (L) or Ade-Cre (C) for 3 days. In all experiments cells were harvested at the indicated times, chromatin fractions prepared and subjected to ChIP analysis of (A and B) the indicated promoter regions or (C) centromere (Cen), subtelomere (Sub-tel), Int N (intergenic regions between *cyclin B1* and *slc30a5*), or Int C (intergenic region between *cyclin B1* and *cenph*). Following precipitation with indicated antibodies, semiquantitative PCR (from 30 to 35 cycles) was used to determine the extent of DNA enrichment.

(D) Model of Chk1-dependent transcriptional repression in response to DNA damage. Under unperturbed conditions, Chk1 associates with chromatin and phosphorylates H3-T11. Phosphorylation of T11 enhances GCN5 recruitment to promoters of relevant genes (*cyclin B1* and *cdk1*) leading to H3-K9 acetylation. In response to DNA damage, Chk1 dissociates from chromatin and H3-T11 becomes dephosphorylated. The decreased phosphorylation at T11 impairs GCN5 recruitment to the promoter, leading to the deacetylation of H3-K9 and reduced transcription.

DISCUSSION

Taken together, the data presented here demonstrate that Chk1 is a histone H3 kinase that regulates transcriptional repression in response to DNA damage. First, Chk1 is capable of phosphorylating nucleosomal histone H3 specifically on residue T11. This demonstrates that Chk1 can efficiently recognize a nucleosome, the subunit structure of chromatin, as a substrate (Figure 3C). Second, Chk1 is chromatin associated under unperturbed conditions (Figure 4A), and the PIKK-mediated DNA-damage-dependent Chk1 chromatin dissociation was prerequisite for concomitant H3-T11 dephosphorylation (Figure 4B). Third, Chk1 depletion resulted in a decrease in phosphorylation of H3-T11 in vivo (Figure 3D).

We used antibodies specific to individual histone modifications to reveal that H3-K9 acetylation was modestly reduced concomitant with the reduction in H3-T11 phosphorylation, in response to both DNA damage (Figure 2) and Chk1 ablation (Figure 3D). H3-K9 acetylation is mediated by GCN5 acetyltransferase and is essential for active transcription. Phosphorylation of H3-T11 was first demonstrated in Rat-1 cells and was reported to be predominantly associated with mitotic chromosomes (Preuss et al., 2003). In the context of our observation that H3-T11 phosphorylation can be readily detected during interphase, this suggested that H3-T11 phosphorylation in addition to H3-S10 phosphorylation has a function in transcriptional regulation. Consistent with this, we clearly demonstrate that H3-T11 phosphorylation significantly enhances the binding affinity between GCN5 HAT and H3 peptides. Thus, changes in the phosphorylation status of H3-T11 in response to DNA damage likely influence GCN5 recruitment at promoters and thus transcription of GCN5-dependent genes.

Although GCN5 was initially reported to acetylate both H3-K9 and H3-K14 (Kuo et al., 1996), GCN5 depletion in mouse and chick cells revealed that while H3-K9 acetylation was significantly reduced, acetylation of H3-K14 remained constant (Bu et al.,

2007; Kikuchi et al., 2005). Here we observed that H3-K9, but not H3-K14, acetylation was always reduced in response to either DNA damage or Chk1 depletion. This was consistent with reduced GCN5 recruitment in these circumstances and the presence of redundant acetyltransferases for H3-K14 as previously suggested (Kouzarides, 2007). An involvement of GCN5 in the mechanism of DNA-damage-dependent transcriptional repression is supported by our ChIP analysis examining the *cyclin B1* and *cdk1* promoter regions (Figure 6). Here we demonstrate that association of Chk1 and the subsequent phosphorylation of H3-T11 were observed at the *GAPDH* promoter region as well as at the promoters of *cyclin B1* and *cdk1*. However, we found that H3-K9 acetylation was only reduced at the *cyclin B1* and *cdk1* promoters after DNA damage or Chk1 depletion but was not changed at the *GAPDH* promoter region. Consistent with this difference, we could not detect GCN5 at the *GAPDH* promoter region under unperturbed conditions but could detect GCN5 at both the *cyclin B1* and *cdk1* promoter regions in unperturbed cells. This suggests that GCN5 is not required for *GAPDH* gene expression (Bu et al., 2007; Kikuchi et al., 2005) but participates in the regulation of *cyclin B1* and *cdk1*. These results suggest that Chk1-dependent changes in H3-K9 acetylation and gene transcription may be dependent on specific DNA-bound transcription factors.

Surprisingly, although Chk1 loss resulted in premature mitosis and a rapid increase in apoptosis in embryonic cells (Liu et al., 2000; Niida et al., 2005; Takai et al., 2000), Chk1 loss resulted in cell-cycle arrest within S phase in somatic MEFs (Figure 5A). In ES cells, Chk1 depletion resulted in loss of the inhibitory Y15 phosphorylation on cdk1 and premature cyclin B1-cdk1 activation. In MEFs, Chk1 depletion also caused loss of inhibitory Y15 phosphorylation on cdk1. The failure to activate cyclin B1-cdk1 and enter premature mitosis is presumably a result of concomitant loss of cyclin B1 and cdk1 proteins (Figure 5B). Irrespective of cell fate, our data clearly demonstrate that Chk1 is required for expression of cyclin B1 and cdk1 and thus for mitotic transitions in MEFs. The rapid proliferation arrest we observed in Chk1-depleted MEFs is consistent with a basal function for Chk1, promoting the expression of a subset of cell-cycle control genes in unperturbed cells. Interestingly, ATR-deficient MEFs divided normally for 1–2 cell cycles after ATR depletion (Brown and Baltimore, 2003). Our results demonstrate that ATR knockdown using specific siRNA prevents the decrease in H3-T11 phosphorylation caused by UV treatment. This would be consistent with our model where the requirement for Chk1 in basal transcription would be independent of ATR function.

The molecular events that underlie the cell-cycle arrest with incomplete DNA replication when Chk1 is depleted remain unknown. It is possible that a number of genes required for DNA replication are transcriptionally repressed when Chk1 is depleted in MEFs. In this regard, Chk1-SA, in which ATR-dependent phosphorylation sites are mutated, can partially suppress several phenotypes observed in Chk1-depleted cells, including *cyclin B1* and *cdk1* expression (even in the presence of DNA damage) and cell-cycle arrest, lending support to this suggestion. We note that GCN5 is utilized as an accessory acetyltransferase for E2Fs, which regulate the expression of the many genes involved in DNA replication (Lang et al., 2001). Furthermore, GCN5 is recruited to the promoters of many cell-cycle genes (Caretti et al., 2003), and GCN5-deficient cells have been shown to exhibit a significant decrease in their growth capability, which is associated with a reduction in the expression of many cell-cycle regulatory genes (Kikuchi et al., 2005). These observations are consistent with GCN5 having a mechanistic role in the repression of transcription following DNA damage and suggest that Chk1 and GCN5 function in the same pathway to regulate the transcription of cell-cycle genes and thus promote cell-cycle progression.

What is the physiological relevance of transcriptional repression in response to DNA damage? We propose that the Chk1-dependent repression of GCN5-dependent gene expression serves as an alternative checkpoint mechanism to promote cell-cycle delay or arrest, in addition to the regulation of inhibitory Y15 phosphorylation of cdk1. The observation that MEFs respond differently from ES cells following Chk1 depletion may suggest that the relative importance of the different Chk1-dependent pathways plays a role in "fine tuning" the DNA-damage response in different cell types. Previous observations that the ectopic expression of both cyclin B1 and cdk1AF can cooperate to abrogate the DNA-damage checkpoint (Jin et al., 1998) remain consistent with our model and observations.

In summary, we propose a model for transcriptional repression in response to DNA damage (Figure 7D). In the absence of DNA damage, Chk1 localizes to chromatin and phosphorylates the T11 residue of histone H3, promoting recruitment of GCN5 to the promoter regions of specific genes. When DNA is damaged or when replication forks are stalled, Chk1 is phosphorylated by the PIKKs, ATR, and ATM, resulting in rapid dissociation from the chromatin. Subsequent dephosphorylation of H3-T11 then results in GCN5 dissociating from the promoter region, leading to a decrease in the acetylation of H3-K9 and subsequent repression of transcription of the target genes. We also observed that Chk1 can phosphorylate other nucleosomal core histone (Figure 3C and data not shown), but the target residue and the physiological role of this phosphorylation remain elusive. Our present results uncover a novel mechanism underlying transcriptional repression in response to DNA damage through phosphorylation of H3 at residue T11.

EXPERIMENTAL PROCEDURES

Establishment of Chk1$^{flox/-}$ MEFs, Treatment with Genotoxic Agents

Chk1$^{flox/-}$ ES cells were generated as described previously (Niida et al., 2005). ES cells were injected into an embryonic day (E) 3.5 blast cyst and transplanted into the uterus of a surrogate mother. The chimeric embryo was harvested at day E13.5 and MEFs from the embryo were prepared. Chimeric MEFs were cultured in G418-containing DMEM with 10% FBS. Immortalized conditional Chk1-deficient MEFs were established by three-month subculture. HCT116 p53$^{-/-}$ cells were cultured in McCoy's 5a medium containing 10% FBS. All cells were cultured at 37°C under 5% CO_2 and treated with either UV (500 J/m^2), IR (10 Gy), bleomycin (40 μg/ml), aphidicolin (5 μM), or nocodazole (0.5 μg/ml).

Immunoblotting

Chromatin fractionation was performed as previously described (Niida et al., 2007). For preparation of whole-cell extracts, cells were lysed in IP kinase buffer (50 mM HEPES, pH 8.0, 150 mM NaCl, 2.5 mM EGTA, 1 mM EDTA 1 mM DTT, 0.1% Tween20, 10% glycerol) containing a cocktail of protease and phosphatase inhibitors. The antibodies used for immunoblotting are shown in the Supplemental Experimental Procedures.

Kinase Assay

Chk1-HA and Chk1-K38M-HA were immunopurified using anti-HA antibodies from infected Sf9 cells. Kinase reactions were performed as described (Niida et al., 2005). Substrates were purified histone H3, core histones prepared as described previously (Tachibana et al., 2002) or nucleosomes prepared with Micrococcus endonuclease as described previously (Sassone-Corsi et al., 1999). For cold reactions, kinase assays were performed without [γ-^{32}P]ATP.

Chromatin Immunoprecipitation Assay

ChIP assays were performed essentially as described (Tachibana et al., 2002). 1×10^7 cells, either irradiated or not with UV or infected with Ade-LacZ or Ade-Cre, were used for the chromatin preparation. Primers used for PCR are shown in the Supplemental Experimental Procedures. Antibodies specific to H3 (ab1791; Abcam), Chk1 (sc-8408; Santa Cruz), pT11 (ab5168; Abcam), AcK9 (ab4441; Abcam), AcK14 (07-353; Upstate), and GCN5 (sc-20698; Santa Cruz) were used for immunoprecipitation.

Knockdown Experiments by siRNA Transfection

HCT116 cells were transfected with a control siRNA (Silencer Negative Control number 1, Ambion 4611) or siRNA for ATR (CCUCCGUGAUGUUGCUUGAtt) using Lipofectamine 2000 (Invitrogen).

Establishing Chk1$^{flox/-}$ MEFs Expressing Chk1 Wild-Type or Chk1-S317A/S345A

Twenty micrograms of pCAGGS-Chk1 wild-type and Chk1-S317A/S345A and 5 μg of PGK-Hyg vector were linearized with SalI and KpnI, respectively. Linearized DNA was electroporated into Chk1$^{flox/-}$ MEFs with a Gene Pulser II. Cells were selected with 0.15 mg/ml hygromycin B for 7 days. Single colonies were screened by immunoblotting with anti-Chk1.

Protein Expression and Purification

Baculoviruses expressing Myc- and His-tagged HAT domains of *S. cerevisiae* GCN5 (residues 100–255) were generated as described previously (Tojima et al., 2000). Human histone H3.1 wild-type or T11 substituted with A was cloned into pET3a, expressed in *E. coli*, and purified as described previously with minor modification (Luger et al., 1999).

Peptide Binding Assay

SPR measurements were performed at 25°C using a Biacore 2000 instrument (Biacore, Inc., Uppsala, Sweden). The HAT domain of *S. cerevisiae* GCN5 was immobilized on the sensor chip CM5 using the amine coupling method according to the manufacturer's instructions. For kinetic measurements, 90 μl of each peptide sample was passed over the sensor surface in the presence or absence of CoA (0.15 mM) at a flow rate of 30 μl/min. The resultant sensor-grams were analyzed using BIAevaluation software (version 4.1).

Supplemental Data

Supplemental Data include Supplemental Experimental Procedures, seven figures, and one table and can be found with this article online at http://www.cell.com/cgi/content/full/132/2/221/DC1/.

ACKNOWLEDGMENTS

We thank Dr. Carr for critical reading of this manuscript, Dr. Katsuno for establishment of Chk1-deficient MEFs, Dr. Mizuno and Dr. Hanaoka for tsFT210 cells, Dr. Nakajima and Dr. Kurimoto for computer analysis, Dr. Osada for discussions, and Dr. Yamada-Namikawa and Miss Kojima for technical assistance. This work was supported in part by the Ministry of Education, Science, Sports, and Culture of Japan through a Grant-in-Aid for Scientific Research (B) awarded to M.N. and for Young Scientists (B) awarded to M.S.

Received: July 19, 2007
Revised: October 17, 2007
Accepted: December 5, 2007
Published: January 24, 2008

REFERENCES

Barlev, N.A., Candau, R., Wang, L., Darpino, P., Silverman, N., and Berger, S.L. (1995). Characterization of physical interactions of the putative transcriptional adaptor, ADA2, with acidic activation domains and TATA-binding protein. J. Biol. Chem. *270*, 19337–19344.

Brown, E.J., and Baltimore, D. (2003). Essential and dispensable roles of ATR in cell cycle arrest and genome maintenance. Genes Dev. *17*, 615–628.

Brownell, J.E., Zhou, J., Ranalli, T., Kobayashi, R., Edmondson, D.G., Roth, S.Y., and Allis, C.D. (1996). Tetrahymena histone acetyltransferase A: a homolog to yeast Gcn5p linking histone acetylation to gene activation. Cell *84*, 843–851.

Bu, P., Evrard, Y.A., Lozano, G., and Dent, S.Y. (2007). Loss of Gcn5 acetyltransferase activity leads to neural tube closure defects and exencephaly in mouse embryos. Mol. Cell. Biol. *27*, 3405–3416.

Caretti, G., Salsi, V., Vecchi, C., Imbriano, C., and Mantovani, R. (2003). Dynamic recruitment of NF-Y and histone acetyltransferases on cell-cycle promoters. J. Biol. Chem. *278*, 30435–30440.

Cheung, P., Tanner, K.G., Cheung, W.L., Sassone-Corsi, P., Denu, J.M., and Allis, C.D. (2000). Synergistic coupling of histone H3 phosphorylation and acetylation in response to epidermal growth factor stimulation. Mol. Cell *5*, 905–915.

Clements, A., Poux, A.N., Lo, W.S., Pillus, L., Berger, S.L., and Marmorstein, R. (2003). Structural basis for histone and phosphohistone binding by the GCN5 histone acetyltransferase. Mol. Cell *12*, 461–473.

Flatt, P.M., Tang, L.J., Scatena, C.D., Szak, S.T., and Pietenpol, J.A. (2000). p53 regulation of G(2) checkpoint is retinoblastoma protein dependent. Mol. Cell. Biol. *20*, 4210–4223.

Gentile, M., Latonen, L., and Laiho, M. (2003). Cell cycle arrest and apoptosis provoked by UV radiation-induced DNA damage are transcriptionally highly divergent responses. Nucleic Acids Res. *31*, 4779–4790.

Grant, P.A., Duggan, L., Cote, J., Roberts, S.M., Brownell, J.E., Candau, R., Ohba, R., Owen-Hughes, T., Allis, C.D., Winston, F., et al. (1997). Yeast Gcn5 functions in two multisubunit complexes to acetylate nucleosomal histones: characterization of an Ada complex and the SAGA (Spt/Ada) complex. Genes Dev. *11*, 1640–1650.

Grant, P.A., Schieltz, D., Pray-Grant, M.G., Yates, J.R., 3rd, and Workman, J.L. (1998). The ATM-related cofactor Tra1 is a component of the purified SAGA complex. Mol. Cell *2*, 863–867.

Jackman, M., Lindon, C., Nigg, E.A., and Pines, J. (2003). Active cyclin B1-Cdk1 first appears on centrosomes in prophase. Nat. Cell Biol. *5*, 143–148.

Jin, P., Hardy, S., and Morgan, D.O. (1998). Nuclear localization of cyclin B1 controls mitotic entry after DNA damage. J. Cell Biol. *141*, 875–885.

Kikuchi, H., Takami, Y., and Nakayama, T. (2005). GCN5: a supervisor in all-inclusive control of vertebrate cell cycle progression through transcription regulation of various cell cycle-related genes. Gene *347*, 83–97.

Kouzarides, T. (2007). Chromatin modifications and their function. Cell *128*, 693–705.

Kramer, A., Mailand, N., Lukas, C., Syljuasen, R.G., Wilkinson, C.J., Nigg, E.A., Bartek, J., and Lukas, J. (2004). Centrosome-associated Chk1 prevents premature activation of cyclin-B-Cdk1 kinase. Nat. Cell Biol. *6*, 884–891.

Kuo, M.H., Brownell, J.E., Sobel, R.E., Ranalli, T.A., Cook, R.G., Edmondson, D.G., Roth, S.Y., and Allis, C.D. (1996). Transcription-linked acetylation by Gcn5p of histones H3 and H4 at specific lysines. Nature *383*, 269–272.

Lang, S.E., McMahon, S.B., Cole, M.D., and Hearing, P. (2001). E2F transcriptional activation requires TRRAP and GCN5 cofactors. J. Biol. Chem. *276*, 32627–32634.

Liu, Q., Guntuku, S., Cui, X.S., Matsuoka, S., Cortez, D., Tamai, K., Luo, G., Carattini-Rivera, S., DeMayo, F., Bradley, A., et al. (2000). Chk1 is an essential kinase that is regulated by Atr and required for the G(2)/M DNA damage checkpoint. Genes Dev. *14*, 1448–1459.

Luger, K., Rechsteiner, T.J., and Richmond, T.J. (1999). Preparation of nucleosome core particle from recombinant histones. Methods Enzymol. *304*, 3–19.

Nilda, H., Tauge, S., Katsuno, Y., Konishi, A., Takeda, N., and Nakanishi, M. (2005). Depletion of Chk1 leads to premature activation of Cdc2-cyclin B and mitotic catastrophe. J. Biol. Chem. *280*, 39246–39252.

Nilda, H., Katsuno, Y., Banerjee, B., Hande, M.P., and Nakanishi, M. (2007). Specific role of Chk1 phosphorylations in cell survival and checkpoint activation. Mol. Cell. Biol. *27*, 2572–2581.

O'Neill, T., Giarratani, L., Chen, P., Iyer, L., Lee, C.H., Bobiak, M., Kanai, F., Zhou, B.B., Chung, J.H., and Rathbun, G.A. (2002). Determination of substrate motifs for human Chk1 and hCds1/Chk2 by the oriented peptide library approach. J. Biol. Chem. *277*, 16102–16115.

Preuss, U., Landsberg, G., and Scheidtmann, K.H. (2003). Novel mitosis-specific phosphorylation of histone H3 at Thr11 mediated by Dlk/ZIP kinase. Nucleic Acids Res. *31*, 878–885.

Rojas, J.R., Trievel, R.C., Zhou, J., Mo, Y., Li, X., Berger, S.L., Allis, C.D., and Marmorstein, R. (1999). Structure of Tetrahymena GCN5 bound to coenzyme A and a histone H3 peptide. Nature *401*, 93–98.

Sassone-Corsi, P., Mizzen, C.A., Cheung, P., Crosio, C., Monaco, L., Jacquot, S., Hanauer, A., and Allis, C.D. (1999). Requirement of Rsk-2 for epidermal growth factor-activated phosphorylation of histone H3. Science *285*, 886–891.

Smits, V.A., Reaper, P.M., and Jackson, S.P. (2006). Rapid PIKK-dependent release of Chk1 from chromatin promotes the DNA-damage checkpoint response. Curr. Biol. *16*, 150–159.

Sterner, D.E., Grant, P.A., Roberts, S.M., Duggan, L.J., Belotserkovskaya, R., Pacella, L.A., Winston, F., Workman, J.L., and Berger, S.L. (1999). Functional organization of the yeast SAGA complex: distinct components involved in structural integrity, nucleosome acetylation, and TATA-binding protein interaction. Mol. Cell. Biol. *19*, 86–98.

Syljuasen, R.G., Sorensen, C.S., Hansen, L.T., Fugger, K., Lundin, C., Johansson, F., Helleday, T., Sehested, M., Lukas, J., and Bartek, J. (2005). Inhibition of human Chk1 causes increased initiation of DNA replication, phosphorylation of ATR targets, and DNA breakage. Mol. Cell. Biol. *25*, 3553–3562.

Tachibana, M., Sugimoto, K., Nozaki, M., Ueda, J., Ohta, T., Ohki, M., Fukuda, M., Takeda, N., Niida, H., Kato, H., and Shinkai, Y. (2002). G9a histone methyltransferase plays a dominant role in euchromatic histone H3 lysine 9 methylation and is essential for early embryogenesis. Genes Dev. *16*, 1779–1791.

Takai, H., Tominaga, K., Motoyama, N., Minamishima, Y.A., Nagahama, H., Tsukiyama, T., Ikeda, K., Nakayama, K., and Nakanishi, M. (2000). Aberrant cell cycle checkpoint function and early embryonic death in Chk1(−/−) mice. Genes Dev. *14*, 1439–1447.

Tojima, Y., Fujimoto, A., Delhase, M., Chen, Y., Hatakeyama, S., Nakayama, K., Kaneko, Y., Nimura, Y., Motoyama, N., Ikeda, K., et al. (2000). NAK is an IkappaB kinase-activating kinase. Nature *404*, 778–782.

Int. J. Cancer: **122,** 1222–1228 (2008)

Susceptibility of p27^{kip1} knockout mice to urinary bladder carcinogenesis induced by *N*-butyl-*N*-(4-hydroxybutyl)nitrosamine may not simply be due to enhanced proliferation

Atsuya Hikosaka[1,2], Kumiko Ogawa[1]*, Satoshi Sugiura[1], Makoto Asamoto[1], Fumitaka Takeshita[1], Shin-Ya Sato[1], Makoto Nakanishi[3], Kenjiro Kohri[2] and Tomoyuki Shirai[1]

[1]*Department of Experimental Pathology and Tumor Biology, Nagoya City University Graduate School of Medical Sciences 1 Kawasumi, Mizuho-cho, Mizuho-ku, Nagoya 467-8601, Japan*
[2]*Department of Nephro-Urology, Nagoya City University Graduate School of Medical Sciences 1 Kawasumi, Mizuho-cho, Mizuho-ku, Nagoya 467-8601, Japan*
[3]*Department of Biochemistry and Cell Biology, Nagoya City University Graduate School of Medical Sciences 1 Kawasumi, Mizuho-cho, Mizuho-ku, Nagoya 467-8601, Japan*

Deregulated proliferation is one of the fundamental characteristics of carcinogenesis. p27 is one of the most well characterized negative cell cycle regulator. In our previous study, expression of p27 protein was found to be dramatically suppressed on stimulation of cell proliferation by calculi in the rodent urinary bladder, withdrawal of the insult resulting in re-expression of p27 and regression of urothelial hyperplastic lesions. In the present study, to evaluate how loss of function impacts on urinary bladder carcinogenesis, *N*-butyl-*N*-(4-hydroxybutyl)nitrosamine (BBN), a bladder carcinogen was given to p27 knockout mice. Males and females with either null, hetero or wild-type p27 alleles were divided into 2 groups, one given drinking water containing 0.05% BBN for 10 weeks and the other receiving distilled water, then, killed at week 20. The experiment was repeated for confirmation of the outcome. In the second experiment, performed with a larger number of animals, the incidence of urinary bladder carcinomas was significantly higher in female p27-null mice than in their wild-type counterparts. p27 deficiency also resulted in their increase of relative weights of urinary bladders and section areas of carcinomas in BBN-treated mice. Interestingly, while BrdU labeling indices generally increased with progression of mucosal proliferative lesions, from normal epithelium, through hyperplasia to carcinoma, there was no significant variation with the p27 genotype, in tumors as well as normal urothelium. These findings suggest that p27 deficient mice have elevated susceptibility to BBN-induction of urinary bladder carcinogenesis through a mechanism which might be independent of acceleration of cell cycling.

Key words: knockout mice; urinary bladder; p27; BBN

Introduction

Failure of cell cycle regulation at different checkpoints is a notable characteristic of carcinogenesis. Cyclins and cyclin-dependent kinases (Cdk) drive the cell cycle whereas Cdk inhibitors such as p27^{kip1}, p21^{waf1}, p16^{INK4a} and p15^{INK4b} act as negative regulators, for example controlling the *Rb* gene phosphorylation status which governs progression from the G1 to the S phase.

The inhibitor p27 belongs to the Cip/Kip family, negatively regulating cyclin D, E and A, and plays a pivotal role in the control of cell proliferation,[1,2] also mediating the growth arrest induced by transforming growth factor β, contact inhibition, growth in suspension, cyclic AMP agonists and other signals.[1,3,4] It is present abundantly and ubiquitously in quiescent cells but declines in proliferating cells in response to mitogenic stimulation by growth factors and cytokines. The concentration of p27 protein is thought to be predominantly regulated by the ubiquitin-proteasome pathway.[5] Cytoplasmic relocalization, also controlled by PKB/Akt-mediated p27 phosphorylation at threonine 157, is considered as an important pathway for p27-induced G1 arrest arrest.[6–8]

Although mutations in the *p27* gene are rare in human tumors,[9–11] decrease or loss of p27 protein correlates with a poor prognosis in breast,[12–14] stomach,[15] colon,[16] ovarian epithelial,[17–19] prostate[20,21] and urinary bladder[22–24] cancers.

In our previous study, protein levels of p27 were found to be slightly decreased in rat hyperplastic urothelial mucosa induced by calculi associated with cell proliferation, then becoming dramatically but reversibly increased after withdrawal of the insult at the same time that the hyperplastic urothelium returned to normal.[25] Similar down and up-regulation of p27 depending on the presence of cell-proliferative stimuli caused by uracil caliculi was also found in carcinogen-induced rat urothelial mucosal hyperplastic lesions, but not in neoplastic lesions such as carcinomas.[25] This fact suggests that disordered expression of p27 plays an important role in urinary bladder carcinogenesis. For further elucidation, we here evaluated alteration of susceptibility to *N*-butyl-*N*-(4-hydroxybutyl)nitrosamine (BBN), a rodent urinary bladder carcinogen, in p27 knockout mice.

Material and methods

Animals

Male p27 heterozygous mice with a targeting construct designed to delete the entire protein-coding region of *p27* gene on one allele[26] were kindly provided by Nippon Roche Research Center (Kamakura, Japan). Following the provider's system, male p27$^{+/-}$ mice were then backcrossed to female C57BL/6 wild mice (Charles River Japan Inc., Atsugi, Japan) for maintenance of the genotype. Subsequently animals for the experiment were obtained by crossing male and female heterozygous p27 mice. They were genotyped with two primer sets: one for wild type *p27* detection; p27-5′, CCT GGA GCG GAT GGA CGC CAG ACA and p27-3′, GCC AGC ACC TTG CAG GCG CTC TTG; and the other for mutant type *p27* (insertion of phosphoglycerate kinase-1) detection; BK1, GGC TAT TGG CTC AAA ACG AAC CTC and MK4, ATG CTC CAG ACT GCC TTG GGA AAA on DNA extracted from tails. Then, they were divided into groups consisting of 6–8 individuals of the same genotype and sex per plastic cage with wooden chips for bedding in an air-conditioned room at

Grant sponsor: Grants-Aid for Cancer Research from the Ministry of Education, Culture, Sports, Science and Technology and the Ministry of Health, Labour and Welfare. Grant sponsor: Grant-in-aid from the Ministry of Health, Labour and Welfare for the Second Term Comprehensive 10-Year Strategy for Cancer Control, Japan. Grant sponsor: Grant from the Society for Promotion of Toxicological Pathology of Nagoya, Japan.

***Correspondence to:** Department of Experimental Pathology and Tumor Biology, Nagoya City University Graduate School of Medical Sciences, 1 Kawasumi, Mizuho-cho, Mizuho-ku, Nagoya 467-8601, Japan.
Fax: +81-52-842-0817. E-mail: kogawa@med.nagoya-cu.ac.jp

Received 2 June 2007; Accepted after revision 19 September 2007
DOI 10.1002/ijc.23249
Published online 20 November 2007 in Wiley InterScience (www.interscience.wiley.com).

22 ± 2°C and 55% ± 5% humidity with a 12 hr light/dark cycle. Tap water and diet were available *ad libitum*.

Animal experiment

To elucidate the possible influence of mixed background strain during the establishment of the knockout mice, experiments were performed twice with different generations. Experiment 1 with 3–10 mice per group and the Experiment 2 with 11–20 mice per group were performed with the 4th and 10th (>90% inbreeding coefficients) generations, respectively, after we received parental animals.

Male and female mice of each p27 genotype, i.e. nullizygous (p27$^{-/-}$), heterozygous (p27$^{+/-}$) and wild (p27$^{+/+}$), at the age of 6–8 weeks were divided into one group given drinking water containing 0.05% BBN (Tokyo Kasei Kogyo Co. Ltd., Tokyo, Japan) for 10 weeks and the other group receiving distilled water (resulting in twelve groups in all). Food and water consumption was monitored once a month and body weights were recorded every week until the end of the experiment. At the 20th experimental week, all mice were killed under ether anesthesia and their urinary bladders, kidneys, livers and spleens were excised. They were weighed and bladders and kidneys were processed for histological examination. One hour before sacrifice in Experiment 2, bromodeoxyuridine (BrdU; Sigma Chemical Co., St. Louis, MO) was injected i.p. into six mice from each group at the dose of 100 mg/kg body weight for assessment of DNA synthesis. The genotype of all animals was confirmed at this point with a DNA sample extracted from the spleen.

Use of the animals in these carcinogenesis experiments was according to the Guidelines for the Care and Use of Laboratory Animals of Nagoya City University Graduate School of Medical Sciences, and was approved by the Institutional Animal Care and Use Committee.

Tissue processing

The urinary bladders were routinely filled with approximately 1 ml of 10% buffered formalin and immersed in the fixative with their necks closed. Those of five mice from each group in Experiment 2 were cut longitudinally into two halves, then one half was frozen in liquid nitrogen and stored at –80°C until DNA extraction and the other was fixed in formalin. Either before or after fixation, bladders were cut in half and weighed. Then, 4–8 longitudinal slices per bladder were made and embedded in paraffin for histological examination. Kidneys were sectioned transversely so that the renal pelvis was available for histological examination after routine processing.

Histo-pathological and immunohistochemical examination

Routine histological examination was performed with hematoxylin and eosin stained sections. Urothelial lesions were classified into simple, papillary or nodular (PN)-hyperplasia or carcinoma, and invasiveness of carcinomas was evaluated as Tis, T1, T2a, T2b and T3 for *in situ*, submucosal, inner half muscular, outer half muscular and extravesical invasion, respectively. In mice, urinary bladder carcinomas generally developed as non-papillary diffuse lesions[27] making it difficult to evaluate tumor multiplicity for the quantitative analysis. In slide sections, areas of carcinoma, recognized as severely atypical urothelium excluding mesenchymal tissue as much as possible were measured with the aid of an image analyzer (Image Processor for Analytical Pathology; Sumika Technoservice, Osaka, Japan). Then, relative values for percentage areas of lesion per total length of urothelium were calculated. For immunohistochemical analyses, anti-BrdU (DAKO Japan, Kyoto, Japan), anti-p27 (C-19; Santa-Cruz Biotechnology, Santa Cruz, CA), anti-p53 (CM-5; Novocastra Laboratories Ltd., Newcastle upon Tyne, UK), anti-p21 (M-19; Santa-Cruz), and anti-cyclin D1 (Immunobiological Laboratories, Gumma, Japan) antibodies were applied at dilutions of 1,000, 500, 800, 25 and 100, respectively. A Vectastain ABC Elite Kit (Vector Laboratories Inc., Burlingame, CA) and diaminobenzidine were used for visualization. For the evaluation of labeling indices of stained nuclei, more than 1,000 urothelial cells per corresponding lesion were counted and percentage values were generated.

Polymerase chain reaction-single strand conformation polymorphism (PCR-SSCP) analyses and direct sequencing

DNA was extracted from frozen bladder tissue specimens, dissolved in 100 µl of water and stored at –20°C. PCR-SSCP analysis was performed to detect mutations in exons 5–8 of the p53 gene, exon sequences being amplified with appropriate oligonucleotide primers as described previously.[28] PCR was carried out in a 10 µl reaction volume containing genomic DNA, 0.4 µM of each primer, 1.6 mM of dNTP mixture, 0.2 mCi of [^{32}P]dCTP (Amersham Biosciences UK Ltd., Buckinghamshire, UK), 2.5 mM of $MgCl_2$, and 10× LA PCR Buffer II (Takara Bio Inc., Otsu, Japan). TaKaRa LA Taq of 0.5 U (Takara Bio) was added and the samples were incubated at 95°C for 5 min followed by 35–40 cycles of amplification in a TaKaRa PCR Thermal Cycler (Takara Bio) with denaturation at 95°C for 45 sec, annealing at 58–62°C for 30 sec and extension at 72°C for 30 sec. Each PCR aliquot was subsequently mixed with 10 µl of stop buffer (98% formamide, 10 mM EDTA, 0.1% bromophenol blue and 0.1% xylene cyanol), heated at 95°C for 3 min, immediately placed on ice and loaded onto a 0.5× MDE gel (Cambrex Bio Science Rockland, Rockland, ME) with or without 5% glycerol. Electrophoresis was performed at 5–8 W for 8 hr. Then the gels were dried and used to expose X-ray film.

To sequence PCR products, the amplified fragments were cut out, eluted from the gels and re-amplified under the same conditions as described above. Electrophoresis of the amplified PCR products was performed in 3% agarose gels, from which DNA amplicons were purified with a QIAquick Gel Extraction Kit (QIAGEN K.K., Tokyo, Japan). Sequencing was performed with a BigDye Terminator Cycle Sequencing Kit and an ABI PRISM 310 Genetic Analyzer according to the supplier's instructions (Applied Biosystems, Foster City, CA).

Statistical analyses

Depending on the size of the group, the Kruskal–Wallis H-test or the Mann–Whitney U-test with the Bonferroni correction were performed for multiple comparisons and the Yates m × n chi-square test was applied for statistical analyses of incidence.

Results

The Experiment 1

Throughout the experimental period, body weight gain was slightly suppressed by BBN-treatment in the male mice of all p27 genotypes. Regardless of the treatment and sex, p27$^{-/-}$ mice tended to show higher body weights than p27$^{+/+}$ mice, with intermediate values obtained for p27$^{+/-}$ mice. The final body weights of p27$^{-/-}$ mice were significantly higher than those of p27$^{+/+}$ mice in untreated males (39.9 ± 1.7 vs. 33.9 ± 4.2 g; $p < 0.05$) and females (31.2 ± 1.6 vs. 22.7 ± 1.1 g; $p < 0.001$) and BBN-treated females (29.3 ± 2.1 vs. 23.6 ± 1.7 g; $p < 0.001$). Although relative urinary bladder weights (‰ of BW) varied greatly in BBN-treated groups averages for –/–, +/– and +/+ mice tended to be higher in BBN-treated groups (15.7 ± 13.6, 5.6 ± 7.5 and 3.4 ± 2.1 in males and 11.7 ± 20.1, 3.8 ± 1.1 and 2.2 ± 0.2 in females, respectively) compared with non-treated groups (1.6 ± 0.6, 1.6 ± 0.3 and 1.5 ± 0.3 in males and 1.8 ± 0.5, 2.1 ± 0.4 and 1.8 ± 0.5 in females, respectively) and p27$^{-/-}$ genotype mice than in non-treated groups and p27$^{+/+}$ genotype mice.

Histological analysis (Table I) showed almost all BBN-treated male mice to have developed urinary bladder carcinomas. In females, 7 out of 7 (100%) with the p27$^{-/-}$ genotype and 2 out of 7 (29%) with the p27$^{+/+}$ genotype developed carcinomas with BBN, these values being significantly different ($p < 0.05$). More-

TABLE I – HISTOPATHOLOGICAL FINDINGS OF THE URINARY BLADDER (THE EXPERIMENT 1)

Genotype of p27	BBN	No. of mice	Incidence (%)					Relative size of carcinoma (mm^2/mm mucosa)
			Hyperplasia		Carcinoma			
			Simple	PN	Non-Invasive	Invasive	Total	
Male								
−/−	+	5	5(100)[3]	5(100)[3]	1(20)	3(60)	4(80)[2]	2.00±2.11
+/−	+	10	10(100)[4]	10(100)[4]	0	9(90)[2]	9(90)[2]	0.25±0.34
+/+	+	7	7(100)[4]	7(100)[4]	1(14)	6(86)[2]	7(100)[2]	0.22±0.49
−/−	−	3	0	0	0	0	0	0
+/−	−	9	0	0	0	0	0	0
+/+	−	7	0	0	0	0	0	0
Female								
−/−	+	7	7(100)[3]	7(100)[3]	2(29)	5(71)[2]	7(100)[1,3]	0.59±1.20
+/−	+	8	8(100)[4]	8(100)[4]	2(25)	3(38)	5(63)	0.04±0.05
+/+	+	7	7(100)[3]	6(86)[3]	0	2(29)	2(29)	0.03±0.07
−/−	−	5	0	0	0	0	0	0
+/−	−	9	0	0	0	0	0	0
+/+	−	5	0	0	0	0	0	0

PN: Papillary or nodular.
[1]Significantly different from +/+ genotype of BBN-treated mice at $p < 0.05$.–[2,3,4]Significantly different from +/+ genotype of untreated mice at $p < 0.05$, 0.01, 0.001, respectively.

over, relative section areas of carcinomas (mm^2/mm mucosal length) tended to be larger with the $p27^{-/-}$ genotype than the $p27^{+/-}$ and $p27^{+/+}$ genotypes in males and females.

The Experiment 2

Body and relative organ weights and macroscopic observation. As shown in Table II, in line with Experiment 1 and the original report for this mouse,[26] increased body weights were found for $p27^{-/-}$ as compared with $p27^{+/+}$ genotype mice as well as elevated relative organ weights for the male liver, kidney and spleen and female spleen (data not shown). BBN-treatment tended to increase the relative urinary bladder weights, and values in the male $p27^{-/-}$ group were significantly higher than in the $p27^{+/+}$ ($p < 0.05$) and $p27^{+/-}$ ($p < 0.05$) cases (Table II). Macroscopically, urinary bladders in BBN-treated mice demonstrated thickening of the wall with mucosal proliferative lesions (Fig. 1). These changes were more obvious in males than in females and were particularly severe in $p27^{-/-}$ male mice.

Histological analysis of the urinary bladder and renal pelvis. Simple hyperplasia or papillary and nodular (PN) hyperplasia, putative premalignant lesions of murine urothelium,[29] occurred in all groups receiving BBN treatment (Table III). Carcinomas were observed in 100, 85 and 80% of male $p27^{-/-}$, $p27^{+/-}$ and $p27^{+/+}$ mice, respectively. The incidences in females were much lower at 38.9, 15.0 and 0%, respectively, with significant variation ($p < 0.05$) among the three p27 genotypes (Table III). Section areas of carcinomas corrected for mucosal length in male and female mice were greater with $p27^{-/-}$ than $p27^{+/+}$, with intermediate values with $p27^{+/-}$ (Table III). Histologically, most of the lesions were characterized as non-papillary type with frequent invasion. More than half of the carcinomas invaded into the muscle layer in male mice, regardless of the p27 genotype. In females, $p27^{-/-}$ mice tended to show a higher incidence of muscle-invading carcinomas than their $p27^{+/-}$ counterparts (Table III).

As shown in Table IV, similar urothelial lesions were also observed in the renal pelvis of BBN-treated mice, simple or PN hyperplasia being observed in 50, 15 and 15%. Moreover, carcinomas were evident in 15.8, 0 and 5.0% of the $p27^{-/-}$, $p27^{+/-}$ and $p27^{+/+}$ male mice, respectively. In females, the incidences were 44.4, 20.0 and 5.6% for simple or PN hyperplasia and 16.7, 5.0 and 0% for carcinomas in the $p27^{-/-}$, $p27^{+/-}$ and $p27^{+/+}$ mice, respectively.

Metastasis was not observed in any major organs in either study.

Immunohistological analysis of the cell cycle in the urinary bladder. BrdU labeling indices tended to be increased in BBN-treated urothelium and apparently reflected the grade of urothelial lesion (Table V). Even though sample number was limited, the indices in untreated normal urothelium, BBN-induced hyperplastic urothelium and carcinoma were similar across the p27 genotype for each category (Table V). The expression pattern of cyclin D1 was found to resemble that of BrdU labeling (data not shown). BrdU-indices were variable in areas of carcinoma, but were generally the same for all genotypes. Immunohistochemical staining for p27 confirmed its lack in $p27^{-/-}$ mice (Figs. 2*a* and 2*d*) and low expression in the urothelium of both $p27^{+/-}$ and $p27^{+/+}$ non-treated mice. In BBN-treated $p27^{+/-}$ and $p27^{+/+}$ mice, expression of p27 was elevated in hyperplastic lesions (Figs. 2*b* and 2*c*), but decreased numbers of positive cells were noted in carcinomas (Figs. 2*e* and 2*f*). p21 expression was apparent in the normal umbrella cells of all $p27^{-/-}$, $p27^{+/-}$ and $p27^{+/+}$ mice, but only a few in BBN-induced carcinoma cells with no compensatory up-regulation in $p27^{-/-}$ mice (Fig. 3). Nuclear expression of p53 was increased in BBN-treated urothelium and apparently reflected the grade of urothelial lesion. However, clear differences across the genotypes were not seen.

SSCP analysis of p53 in urinary bladder carcinomas. As summarized in Table VI, point mutations in the p53 gene (exon5-exon8) were detected by SSCP analysis in 2 of 5 (40%), 1 of 3 (33%) and 1 of 3 (33%) urothelial carcinomas in BBN-treated male mice with the $p27^{-/-}$, $p27^{+/-}$ and $p27^{+/+}$ genotypes, respec-

TABLE II – BODY AND RELATIVE BLADDER WEIGHTS

Genotype of p27	BBN	No. of mice	Final body weight (g)	Relative bladder weight (‰)
Male				
−/−	+	19	34.1 ± 2.5[1,3]	16.3 ± 22.6[2,4]
+/−	+	20	31.1 ± 1.6	4.5 ± 5.1
+/+	+	20	30.6 ± 2.8	3.0 ± 1.5
−/−	−	14	34.7 ± 2.1[2,4]	1.7 ± 0.5
+/−	−	13	31.9 ± 2.7	1.9 ± 0.5
+/+	−	15	31.8 ± 3.1	1.5 ± 0.6
Female				
−/−	+	18	29.5 ± 3.2[1,3]	2.7 ± 1.5
+/−	+	20	26.5 ± 2.2	2.4 ± 0.8
+/+	+	18	24.2 ± 1.8	2.1 ± 0.5
−/−	−	11	31.3 ± 2.3[1,3]	1.5 ± 0.6
+/−	−	15	26.3 ± 2.0[2]	1.9 ± 0.6
+/+	−	15	24.0 ± 2.6	2.0 ± 0.6

Data are means ± SD values.
[1,2]$p < 0.01$, 0.05 vs +/+ group (of the same treatment), respectively.–[3,4]$p < 0.01$, 0.05 vs +/− group (of the same treatment), respectively.

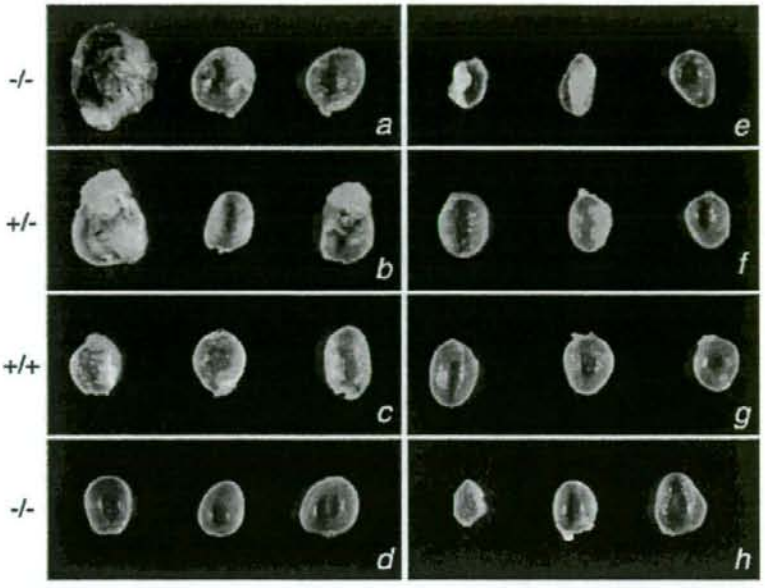

FIGURE 1 – Representative macroscopic appearance of urinary bladders in Experiment 2. BBN-treated urinary bladders in males (*a–c*) and females (*e–g*) are rough in surface, compared with the non-treated male (*d*) and female (*h*) controls. Larger tumors are evident in −/− (*a* and *e*) than +/+ (*c* and *g*) in both sexes. Animals with the +/− genotype (*b* and *f*) also have relatively large tumors.

TABLE III – HISTOPATHOLOGICAL FINDINGS OF THE URINARY BLADDER (THE EXPERIMENT 2)

Genotype of p27	No. of mice	Simple or PN hyperplasia[1] (%)	Carcinoma						Relative size of carcinoma (mm²/mm mucosa)
			Tis	T1	T2a	T2b	T3	Total (%)	
Male									
−/−	19	11 (100)[2]	0	7	3	5	4	19 (100)	0.64 ± 0.72
+/−	20	15 (100)	2	6	4	4	1	17 (85.0)	0.37 ± 0.62
+/+	20	15 (100)	2	5	4	2	3	16 (80.0)	0.13 ± 0.15
Female									
−/−	18	13 (100)	1	1	3	2	0	7 (38.9)[3]	0.26 ± 0.20
+/−	20	15 (100)	0	2	1	0	0	3 (15.0)[3]	0.03 ± 0.02
+/+	18	13 (100)	0	0	0	0	0	0[3]	0

Tis: carcinoma in situ, T1: submucosal invasion, T2a: inner half muscular invasion, T2b: outer half muscular invasion, T3: extravesical invasion, PN: papillary or nodular.
[1]5 cases for frozen specimens were excluded in each group.–[2]3 dead cases were additionally excluded.–[3]Significantly different among genotypes at $p < 0.05$.

tively. One was a silent mutation and no particular pattern was evident. Mutations were not detected in PN hyperplasia of BBN-treated male mice or in either carcinomas or PN hyperplasia of BBN-treated female mice.

Discussion

The present duplicated experiment revealed that p27 deficiency enhances susceptibility to BBN-induction of urinary bladder carcinogenesis in mice. Significant genotype differences were thus noted in the incidences of carcinoma in the females or relative section areas of carcinoma/bladder weight in the males. It has been reported that p27 is haplo-insufficient for tumor suppression.[30] The values in heterozygous animals of our study were also between wild and deficient genotypes, but, relatively close to those for the wild type.

Interestingly, while BrdU labeling indices were generally elevated with progression of mucosal proliferative lesions, from normal epithelium through hyperplasia to carcinoma, there was no significant variation among the p27 genotypes. A similar tendency was seen for cyclin D1-labeling indices (data not shown). These facts suggest that p27 deficiency does not simply increase cell pro-

TABLE IV – INCIDENCE OF RENAL PELVIC NEOPLASIA

Genotype of p27	No. of mice	Simple or PN hyperplasia[1] (%)	Carcinoma				
			Tis	T1	T2	T3	Total(%)
Male							
−/−	16[1]	8 (50.0)	0	1	1	1	3 (15.8)
+/−	20	3 (15.0)	0	0	0	0	0
+/+	20	3 (15.0)	0	1	0	0	1 (5.0)
Female							
−/−	18	8 (44.4)	0	1	1	1	3 (16.7)
+/−	20	4 (20.0)	0	0	0	1	1 (5.0)
+/+	18	1 (5.6)	0	0	0	0	0

Tis: carcinoma in situ, T1: submucosal invasion, T2: muscular invasion, T3: renal parenchymal invasion, PN: papillary or nodular.
[1]Dead cases were excluded.

TABLE V – BRDU LABELING INDICES OF URINARY BLADDER LESION(%)

Genotype of p27	BBN	Normal	Simple hyperplasia	PN hyperplasia	Carcinoma
Male					
−/−	+		(4) 1.85 ± 0.65	(4) 4.56 ± 1.71	(6) 6.37 ± 5.40
+/−	+	(1) 0.29	(4) 1.56 ± 1.64	(6) 5.02 ± 2.19	(6) 10.9 ± 4.66
+/+	+		(3) 1.02 ± 0.90	(5) 5.38 ± 1.99	(6) 11.3 ± 2.48
−/−	−	(6) 0.10 ± 0.09			
+/−	−	(6) 0.08 ± 0.12			
+/+	−	(6) 0.10 ± 0.11			
Female					
−/−	+	(3) 0.30 ± 0.30	(4) 0.63 ± 0.70	(3) 1.46 ± 0.68	(1) 11.97
+/−	+	(3) 0.36 ± 0.34	(5) 0.98 ± 0.55	(4) 3.82 ± 2.99	(1) 6.77
+/+	+	(2) 0 ± 0	(5) 0.22 ± 0.07	(3) 2.43 ± 1.47	(1) 8.93
−/−	−	(6) 0.09 ± 0.10			
+/−	−	(6) 0.11 ± 0.10			
+/+	−	(6) 0.03 ± 0.05			

( ): Effective number of mice for each lesion. PN: papillary or nodular.

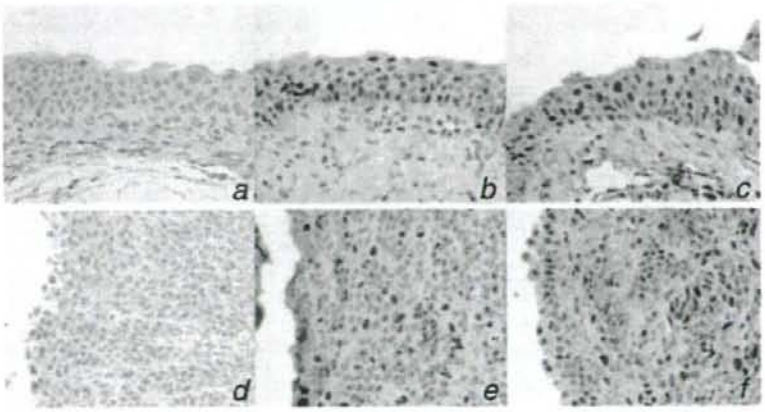

FIGURE 2 – Representative immunohistochemical staining for p27 in BBN-induced urinary bladder hyperplasia (*a–c*) and carcinomas (*d–f*) of male mice. p27 null (−/−: *a*, *d*) mice lack p27 as expected. p27 hetero (+/−: *b*, *e*) and wild (+/+: *c*, *f*) mice express p27 in a relatively high proportion of urothelial nuclei in hyperplasia and to a lesser extent in carcinomas. Slightly weaker staining was observed in hetero than in wild type mice.

liferation and that other parameters pertinent to regulation of cell cycle and tumor growth might be involved.

p27 inactivation has been reported as an independent prognostic marker in various human cancers, correlating with higher tumor grade and poor survival.[12–24] Detailed evaluation of clinical cases of urinary bladder carcinomas revealed a correlation of low p27 expression with high tumor grade and reduced disease-free survival in primary superficial cancers[22] as well as increased muscle invasion and lymph node metastasis.[23,24] On the other hand, Doganay *et al.*, provided evidence that expression of p27 is generally low in urinary bladder carcinoma but is not related to tumor grade, stage, PCNA index, recurrence rate and prognosis. They concluded that p27 expression may not be an independent predictor of outcome with transitional cell carcinoma of the urinary bladder.[31]

In a previous study using a chemically induced skin carcinogenesis model in p27 knockout mice, the mean number of papillomas per mice did not differ between the p27 genotypes, but the incidence for papillomas > 5 mm in size in p27 null mice was 3.3 times higher than in the wild-type,[32] pointing to rapid clonal expansion of initiated cells during promotion. A similar result was reported in the tumors of salivary and mammary gland in $p27^{-/-}$ mice compared with in $p27^{+/+}$ mice carrying the MMTV/v-Ha-*ras* transgene.[33]

In our experiment, due to the morphological characteristics of non-papillary and invasive BBN-induced mouse urinary bladder carcinomas,[27] we could not evaluate the numbers of tumors per mice. Even though the degree of muscle invasion or histology of carcinomas did not statistically differ with the p27 genotype status, the tumor size tended to be larger with the $p27^{-/-}$ genotype. p27 expression in both $p27^{+/-}$ and $p27^{+/+}$ mice was also decreased in BBN-induced urinary bladder carcinomas as compared with premalignant hyperplastic lesions, similar to the decrease observed earlier in F344 rats.[25] This fact points to the cross-species broad importance of p27 in the urinary bladder carcinogenesis.

Combined with the fact that p27 deficiency does not cause significant cell cycle enhancement and does increase tumor volume, our data suggest that the onset of the tumor might be earlier in $p27^{-/-}$ mice than $p27^{+/+}$ littermate. Thus, p27 may act mainly as a tumor suppressor in the early period of carcinogenesis.

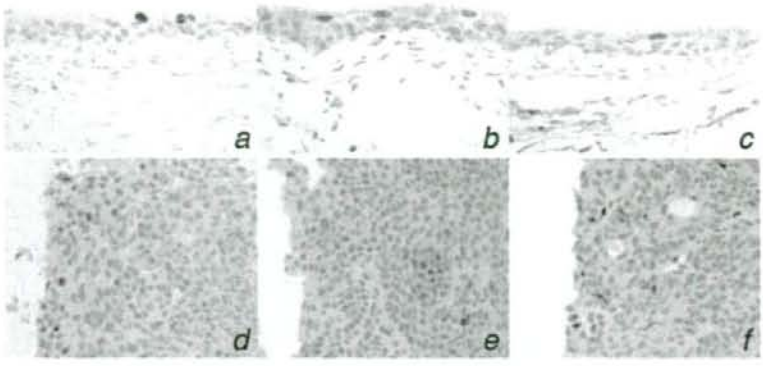

FIGURE 3 – Representative immunohistochemical staining for p21 in non-treated control urinary bladder (*a–c*) and BBN-induced carcinomas (*d–f*) of male mice. Note positive nuclear staining in normal umbrella cells and a few carcinoma cells with no obvious difference among p27 genotypes; null (*–/–*: *a*, *d*), hetero (*+/–*: *b*, *e*) and wild-type (*+/+*: *c*, *f*).

TABLE VI – INCIDENCE OF P53 MUTATION IN BBN-TREATED MICE URINARY BLADDER TISSUE AND MUTATION STATUS

Genotype of p27	Incidence (%)		Mutation status				
	Ca	PN	Case	Lesion	Exon	Codon	Base (amino acid) change
Male							
–/–	2/5 (40)	0	101	Ca (T2b)	6	213	GTG (Leu)→GCG (Ala)
					7	252	ATC (Ile)→AGC (Ser)
			105	Ca (T2b)	8	297	CCC (Pro)→CCT (Pro)
+/–	1/3 (33.3)	0/2	505	Ca (T2b)	7	245	CGC (Arg)→TGC (Cys)
					8	275	CCT (Pro)→ACT (Thr)
					8	301	GCA (Ala)→GGA (Gly)
+/+	1/3 (33.3)	0/2	903	Ca (T2a)	5	132	TGC (Cys)→TGG (Trp)
Female							
–/–	0/3	0/2					
+/–	0/1	0/1					
+/+	0	0					

Ca: carcinoma, PN: papillary or nodular hyperplasia, T2a: inner half muscular invasion, T2b: outer half muscular invasion.

p27 deficiency has been reported to be a key event in the pathogenesis of prostate cancer as indicated by the short latency and complete penetrance in $Pten^{+/-}$ mice.[34] Furthermore, in mice expressing the SV40 large T antigen under control of the androgen receptor dependent-probasin promoter, p27 deficiency did not increase the cell proliferation index or reduce the apoptotic index, but was associated with progression of prostate tumors from high-grade prostatic intraepithelial neoplasia to poorly differentiated carcinomas.[35] Germ-line mutations in p27 have been identified as responsible for a multiple endocrine neoplasia syndrome in rats and humans.[36] Altered expression of p21, another member of Cip/Kip family or its upstream factor, p53, were not observed in either $p27^{+/-}$ or $p27^{-/-}$ mice in the present study. It was also reported that knockdown of p27 with siRNA p21 in epithelial cells did not effect p21 expression, the BrdU-labeling indices or the percentage of cells entering S phase.[37] The rate for p53 mutations in urothelial carcinomas was not increased in our $p27^{-/-}$ mice, although loss of nuclear p27 in human colorectal cancer is reported to be correlated with microsatellite instability and CpG island methylator phenotype.[38] Therefore p27 may have tumor suppressive functions besides its role in cell cycle regulation and p53-p21 pathway. In the mouse urothelium, p27 is normally expressed in the nucleus, but there is accumulating evidence that cytoplasmic relocalization of p27 protein due to PKB/Akt-mediated phosphorylation, an alternative regulation pathway of p27 inactivation, plays an important role in human tumors, such as breast cancers[6–8] and acute myelogenous leukemia.[39] Recent study using $p27^{CK-}$ mice, which carries two point mutations both in the cyclin-binding domain and the CDK-binding domain, showed cytoplasmic localization of p27 was potentially oncogenic through a cyclin-CDK-independent function.[40] Thus we hypothesize that loss of nuclear p27 accelerates mice urinary bladder carcinogenesis, but the mechanistic pathway and impact of p27 expression may differ with the organ or depend on the status of other factors.

In conclusion, p27 deficiency appears to promote BBN-induced urinary bladder carcinogenesis in p27 knockout mice, in line with the poor prognosis of $p27^{-/-}$ clinical bladder carcinomas and this promotion may not simply be related to cell cycle acceleration.

References

1. Polyak K, Lee M-H, Erdjument-Bromage H, Koff A, Roberts JM, Tempst P, Massagué J. Cloning of $p27^{Kip1}$, a cyclin-dependent kinase inhibitor and a potential mediator of extracellular antimitogenic signals. Cell 1994;78:59–66.
2. Toyoshima H, Hunter T. p27, a novel inhibitor of G1 cyclin-Cdk protein kinase activity, is related to p21. Cell 1994;78:67–74.
3. Kato JY, Matsuoka M, Polyak K, Massague J, Sherr CJ. Cyclic AMP-induced G1 phase arrest mediated by an inhibitor (p27Kip1) of cyclin-dependent kinase 4 activation. Cell 1994;79:487–96.
4. Sherr CJ, Roberts JM. CDK inhibitors: positive and negative regulators of G1-phase progression. Genes Dev 1999;13:1501–12.
5. Pagano M, Tam SW, Theodoras AM, Beer-Romero P, Del Sal G, Chau V, Yew PR, Draetta GF, Rolfe M. Role of the ubiquitin-proteasome pathway in regulating abundance of the cyclin-dependent kinase inhibitor p27. Science 1995;269:682–5.
6. Viglietto G, Motti ML, Bruni P, Melillo RM, D'Alessio A, Califano D, Vinci F, Chiappetta G, Tsichlis P, Bellacosa A, Fusco A, Santoro M. Cytoplasmic relocalization and inhibition of the cyclin-dependent kinase inhibitor p27(Kip1) by PKB/Akt-mediated phosphorylation in breast cancer. Nat Med 2002;8:1136–44.
7. Shin I, Yakes FM, Rojo F, Shin NY, Bakin AV, Baselga J, Arteaga CL. PKB/Akt mediates cell-cycle progression by phosphorylation of p27(Kip1) at threonine 157 and modulation of its cellular localization. Nat Med 2002;8:1145–52.
8. Liang J, Zubovitz J, Petrocelli T, Kotchetkov R, Connor MK, Han K, Lee JH, Ciarallo S, Catzavelos C, Beniston R, Franssen E, Slingerland JM. PKB/Akt phosphorylates p27, impairs nuclear import of p27 and opposes p27-mediated G1 arrest. Nat Med 2002;8:1153–60.
9. Pietenpol JA, Bohlander SK, Sato Y, Papadopoulos N, Liu B, Friedman C, Trask BJ, Roberts JM, Kinzler KW, Rowley JD, Vogelstein B. Assignment of the human $p27^{Kip1}$ gene to 12p13 and its analysis in leukemias. Cancer Res 1995;55:1206–10.
10. Ponce-Castañeda MV, Lee M-H, Latres E, Polyak K, Lacombe L, Montgomery K, Mathew S, Krauter K, Sheinfeld J, Massague J, Cordon-Cardo C. $p27^{Kip1}$: chromosomal mapping to 12p12-12p13.1 and absence of mutations in human tumors. Cancer Res 1995;55: 1211–4.
11. Spirin KS, Simpson JF, Takeuchi S, Kawamata N, Miller CW, Koeffler HP. *p27/Kip1* mutation found in breast cancer. Cancer Res 1996;56:2400–4.
12. Catzavelos C, Bhattacharya N, Ung YC, Wilson JA, Roncari L, Sandhu C, Shaw P, Yeger H, Morava-Protzner I, Kapusta L, Franssen E, Pritchard KI, et al. Decreased levels of the cell-cycle inhibitor $p27^{Kip1}$ protein: prognostic implications in primary breast cancer. Nature Med 1997;3:227–30.
13. Porter PL, Malone KE, Heagerty PJ, Alexander GM, Gatti LA, Firpo EJ, Daling JR, Roberts JM. Expression of cell-cycle regulators $p27^{Kip1}$ and cyclin E, alone and in combination, correlate with survival in young breast cancer patients. Nat Med 1997;3:222–5.
14. Tan P, Cady B, Wanner M, Worland P, Cukor B, Magi-Galluzzi C, Lavin P, Draetta G, Pagano M, Loda M. The cell cycle inhibitor p27 is an independent prognostic marker in small ($T_{1a,b}$) invasive breast carcinomas. Cancer Res 1997;57:1259–63.
15. Mori M, Mimori K, Shiraishi T, Tanaka S, Ueo H, Sugimachi K, Akiyoshi T. p27 expression and gastric carcinoma. Nat Med 1997; 3:593.
16. Loda M, Cukor B, Tam SW, Lavin P, Fiorentino M, Draetta GF, Jessup JM, Pagano M. Increased proteasome-dependent degradation of the cyclin-dependent kinase inhibitor p27 in aggressive colorectal carcinomas. Nature Med 1997;3:231–4.
17. Newcomb EW, Sosnow M, Demopoulos RI, Zeleniuch-Jacquotte A, Sorich J, Speyer JL. Expression of the cell cycle inhibitor p27KIP1 is a new prognostic marker associated with survival in epithelial ovarian tumors. Am J Pathol 1999;154:119–25.
18. Sui L, Tokuda M, Ohno M, Hatase O, Hando T. The concurrent expression of p27(kip1) and cyclin D1 in epithelial ovarian tumors. Gynecol Oncol 1999;73:202–9.
19. Masciullo V, Sgambato A, Pacilio C, Pucci B, Ferrandina G, Palazzo J, Carbone A, Cittadini A, Mancuso S, Scambia G, Giordano A. Frequent loss of expression of the cyclin-dependent kinase inhibitor p27 in epithelial ovarian cancer. Cancer Res 1999;59:3790–4.
20. Tsihlias J, Kapusta LR, DeBoer G, Morava-Protzner I, Zbieranowski I, Bhattacharya N, Catzavelos GC, Klotz LH, Slingerland JM. Loss of cyclin-dependent kinase inhibitor $p27^{Kip1}$ is a novel prognostic factor in localized human prostate adenocarcinoma. Cancer Res 1998;58: 542–8.
21. Cote RJ, Shi Y, Groshen S, Feng AC, Cordon-Cardo C, Skinner D, Lieskovosky G. Association of p27Kip1 levels with recurrence and survival in patients with stage C prostate carcinoma. J Natl Cancer Inst 1998;90:916–20.
22. Sgambato A, Migaldi M, Faraglia B, Garagnani L, Romano G, De Gaetani C, Ferrari P, Capelli G, Trentini GP, Cittadini A. Loss of $p27^{Kip1}$ expression correlates with tumor grade and with reduced disease-free survival in primary superficial bladder cancers. Cancer Res 1999;59:3245–50.
23. Korkolopoulou P, Christodoulou P, Konstantinidou AE, Thomas-Tsagli E, Kapralos P, Davaris P. Cell cycle regulators in bladder cancer: a multivariate survival study with emphasis on p27Kip1. Hum Pathol 2000;31:751–60.
24. Kamai T, Takagi K, Asami H, Ito Y, Oshima H, Yoshida KI. Decreasing of $p27^{Kip1}$ and cyclin E protein levels is associated with progression from superficial into invasive bladder cancer. Br J Cancer 2001;84:1242–51.
25. Ogawa K, Kimoto N, Asamoto M, Nakanishi M, Takahashi S, Shirai T. Aberrant expression of $p27^{Kip1}$ is associated with malignant transformation of the rat urinary bladder epithelium. Carcinogenesis 2000;21:117–21.
26. Nakayama K, Ishida N, Shirane M, Inomata A, Inoue T, Shishido N, Horii I, Loh DY, Nakayama K-I. Mice lacking $p27^{Kip1}$ display increased body size, multiple organ hyperplasia, retinal dysplasia, and pituitary tumors. Cell 1996;85:707–20.
27. Cohen SM. Comparative pathology of proliferative lesions of the urinary bladder. Toxicol Pathol 2002;30:663–71.
28. Ogawa K, Uzvolgyi E, St. John MK, de Oliveira ML, Arnold L, Cohen SM. Frequent *p53* mutations and occasional loss of chromosome 4 in invasive bladder carcinoma induced by *N*-butyl-*N*-(4-hydroxybutyl)nitrosamine in B6D2F1 mice. Mol Carcinog 1998;21: 70–9.
29. Fukushima S, Imaida K, Sakata T, Okamura T, Shibata M-A, Ito N. Promoting effects of sodium L-ascorbate on two-stage urinary bladder carcinogenesis in rats. Cancer Res 1983;43:4454–7.
30. Fero ML, Randel E, Gurley KE, Roberts JM, Kemp CJ. The murine gene $p27^{Kip1}$ is haplo-insufficient for tumor suppression. Nature 1998;396:177–80.
31. Doganay L, Altaner S, Bilgi S, Kaya E, Ekuklu G, Kutlu K. Expression of the cyclin-dependent kinase inhibitor p27 in transitional cell bladder cancers: is it a good predictor for tumor behavior? Int Urol Nephrol 2003;35:181–8.
32. Philipp J, Vo K, Gurley KE, Seidel K, Kemp CJ. Tumor suppression by p27Kip1 and p21Cip1 during chemically induced skin carcinogenesis. Oncogene 1999;18:4689–98.
33. Jackson RJ, Adnane J, Coppola D, Cantor A, Sebti SM, Pledger WJ. Loss of the cell cycle inhibitors p21(Cip1) and p27(Kip1) enhances tumorigenesis in knockout mouse models. Oncogene 2002;21:8486–97.
34. Di Cristofano A, De Acetis M, Koff A, Cordon-Cardo C, Pandolfi PP. Pten and p27KIP1 cooperate in prostate cancer tumor suppression in the mouse. Nat Genet 2001;27:222–4.
35. Shaffer DR, Viale A, Ishiwata R, Leversha M, Olgac S, Manova K, Satagopan J, Scher H, Koff A. Evidence for a p27 tumor suppressive function independent of its role regulating cell proliferation in the prostate. Proc Natl Acad Sci USA 2005;102:210–5.
36. Pellegata NS, Quintanilla-Martinez L, Siggelkow H, Samson E, Bink K, Höfler H, Fend F, Graw J, Atkinson MJ. Germ-line mutations in $p27^{Kip1}$ cause a multiple endocrine neoplasia syndrome in rats and humans. Proc Natl Acad Sci USA 2006;103:15558–63.
37. Bryant P, Zheng Q, Pumiglia K. Focal adhesion kinase controls cellular levels of p27/Kip1 and p21/Cip1 through Skp2-dependent and -independent mechanisms. Mol Cell Biol 2006;26:4201–13.
38. Ogino S, Kawasaki T, Kirkner GJ, Yamaji T, Loda M, Fuchs CS. Loss of nuclear p27 (CDKN1B/KIP1) in colorectal cancer is correlated with microsatellite instability and CIMP. Mod Pathol 2007;20: 15–22.
39. Min YH, Cheong JW, Kim JY, Eom JI, Lee ST, Hahn JS, Ko YW, Lee MH. Cytoplasmic mislocalization of p27Kip1 protein is associated with constitutive phosphorylation of Akt or protein kinase B and poor prognosis in acute myelogenous leukemia. Cancer Res 2004; 64:5225–31.
40. Besson A, Hwang HC, Cicero S, Donovan SL, Gurian-West M, Johnson D, Clurman BE, Dyer MA, Roberts JM. Discovery of an oncogenic activity in $p27^{Kip1}$ that causes stem cell expansion and a multiple tumor phenotype. Genes Dev 2007;21:1731–46.

The EMBO Journal (2008) 27, 132–142 | © 2008 European Molecular Biology Organization | All Rights Reserved 0261-4189/08
www.embojournal.org

THE EMBO JOURNAL

Cdc2p controls the forkhead transcription factor Fkh2p by phosphorylation during sexual differentiation in fission yeast

Midori Shimada[1], Chisato Yamada-Namikawa[1], Yuko Murakami-Tonami[1], Takashi Yoshida[1], Makoto Nakanishi[1], Takeshi Urano[2] and Hiroshi Murakami[1,*]

[1]Department of Biochemistry and Cell Biology, Graduate School of Medicine, Nagoya City University, Mizuho-ku, Nagoya, Japan and [2]Department of Biochemistry II, Graduate School of Medicine, Nagoya University, Showa-ku, Nagoya, Japan

In most eukaryotes, cyclin-dependent kinases (Cdks) play a central role in control of cell-cycle progression. Cdks are inactivated from the end of mitosis to the start of the next cell cycle as well as during sexual differentiation. The forkhead-type transcription factor Fkh2p is required for the periodic expression of many genes and for efficient mating in the fission yeast *Schizosaccharomyces pombe*. However, the mechanism responsible for coordination of cell-cycle progression with sexual differentiation is still unknown. We now show that Fkh2p is phosphorylated by Cdc2p (Cdk1) and that phosphorylation of Fkh2p on T314 or S462 by this Cdk blocks mating in *S. pombe* by preventing the induction of *ste11*$^+$ transcription, which is required for the onset of sexual development. We propose that functional interaction between Cdks and forkhead transcription factors may link the mitotic cell cycle and sexual differentiation.

The EMBO Journal (2008) **27**, 132–142. doi:10.1038/sj.emboj.7601949; Published online 6 December 2007
Subject Categories: cell cycle
Keywords: Cdk1; development; phosphorylation; transcription factor; cell cycle

Introduction

The mechanism responsible for the switch from growth to sexual development has been studied in many organisms including the fission yeast *Schizosaccharomyces pombe*. In fission yeast, the onset of sexual development requires both a pheromone signal and the depletion of nutrients, especially that of nitrogen (Yamamoto, 1996; Yamamoto *et al*, 1997). If cells of the opposite mating type are available, those that have committed to sexual development conjugate to form diploids. These diploid cells then undergo meiosis and complete sexual development.

The transcription factor Ste11p plays a central role in commitment to sexual development in fission yeast (Sugimoto *et al*, 1991; Yamamoto, 1996; Yamamoto *et al*, 1997). It regulates the transcription of many genes required for the initiation and progression of conjugation and meiosis (Mata and Bähler, 2006; Xue-Franzen *et al*, 2006). Expression of *ste11*$^+$ itself is regulated by several pathways (Yamamoto, 1996; Yamamoto *et al*, 1997), including the cyclic AMP (cAMP) pathway. Nutrient exhaustion results in a decrease in the intracellular concentration of cAMP and a consequent inactivation of cAMP-dependent protein kinase (PKA). The transcriptional activator Rst2p, which is negatively regulated by PKA, then binds to the upstream region of *ste11*$^+$ and induces the production of *ste11*$^+$ mRNA (Kunitomo *et al*, 2000; Higuchi *et al*, 2002). In addition, a stress signal mediated by the mitogen-activated protein kinase pathway is required for the induction of *ste11*$^+$ mRNA in response to nutrient deprivation (Takeda *et al*, 1995; Kato *et al*, 1996; Shiozaki and Russell, 1996). In addition to the regulation of *ste11*$^+$ transcription, the activity of the encoded protein (Ste11p) is regulated at a post-translational level (Li and McLeod, 1996; Kitamura *et al*, 2001; Qin *et al*, 2003; Kjaerulff *et al*, 2005).

In fission yeast, the single cyclin-dependent kinase (Cdk) Cdc2p controls cell-cycle progression in a manner dependent on various internal and external conditions including nutrient availability (MacNeill and Nurse, 1997). Both nitrogen starvation and pheromone induce arrest in G_1 phase of the cell cycle by inhibiting the activity of Cdc2p, an effect in turn mediated by cyclin degradation and upregulation of Cdk inhibitors. Pheromone induces degradation of the B-type cyclins Cig2p and Cdc13p as well as upregulation of the Cdk inhibitor Rum1p (Stern and Nurse, 1997, 1998). Nitrogen exhaustion also promotes the degradation of both Cig2p and Cdc13p by activating the anaphase-promoting complex (Yamaguchi *et al*, 1997; Kitamura *et al*, 1998; Yamano *et al*, 2004). Linkage between cell-cycle control and sexual development is likely provided by Cig2p. Loss of Cig2p function promotes mating, whereas overproduction of this cyclin negatively regulates sexual differentiation (Obara-Ishihara and Okayama, 1994).

Members of the forkhead-box family of transcription factors are present in almost all eukaryotes (Costa, 2005; Costa *et al*, 2005; Wang *et al*, 2005). More than 50 such proteins that share homology in the winged-helix DNA-binding domain have been identified in higher eukaryotes. This family of transcription factors is implicated in the regulation of a variety of cellular processes, including the cell cycle, apoptosis, DNA repair, stress resistance, and metabolism. The Sanger Center database (http://www.sanger.ac.uk/) indicates the existence of four forkhead proteins in fission

*Corresponding author. Department of Biochemistry and Cell Biology, Graduate School of Medicine, Nagoya City University, 1 Kawasumi, Mizuho-cho, Nagoya, Aichi 467-0001, Japan.
Tel.: +81 52 853 8145; Fax: +81 52 842 3955;
E-mail: hmura@med.nagoya-cu.ac.jp

Received: 24 June 2007; accepted: 15 November 2007; published online: 6 December 2007

yeast: Fkh2p, Fhl1p, Sep1p, and Mei4p (Bahler, 2005). Fkh2p is required for efficient G_2–M transition, normal septation, and periodic gene expression (Buck *et al*, 2004; Bulmer *et al*, 2004; Rustici *et al*, 2004; Szilagyi *et al*, 2005). It is also required for efficient mating (Szilagyi *et al*, 2005). However, the mechanism responsible for the partial sterile phenotype of *fkh2* mutant cells has remained unknown.

We have now investigated the role of Cdc2p in coordination of cell-cycle control and sexual differentiation in fission yeast. We show here that the forkhead transcription factors, including Fkh2p, are responsible for mediating a signal from the kinase Cdc2p to the transcription factor Ste11p.

Results

Forkhead transcription factors are required for mating

Fkh2p, Fhl1p, Mei4p, and Sep1p are the forkhead transcription factors in fission yeast. Given that *fkh2*-deleted cells show a partial sterile phenotype (Szilagyi *et al*, 2005), we investigated the role of forkhead transcription factors in mating in fission yeast. We constructed homothallic strains in which each gene for the forkhead transcription factors was individually deleted. Consistent with previous observations (Ribar *et al*, 1999), *sep1*-deleted cells manifested a pronounced septation defect and slow growth. We, therefore, did not further characterize the role of *sep1*$^+$ in mating. In addition to *fkh2*-deleted cells, we found that *fhl1*-deleted and unexpectedly *mei4*-deleted cells exhibited a partial sterile phenotype, whereas *fkh2 fhl1*, *fkh2 mei4* and *fhk2 fhl1 mei4* mutant cells showed a more pronounced sterile phenotype than did cells lacking either gene alone (Figure 1A). These results suggested that, among the forkhead transcription factors, Fkh2p plays the predominant role in mating, with Fhl1p and Mei4p having minor roles that partially overlap with that of Fkh2p.

Given that the induction of *ste11*$^+$ mRNA plays a central role in mating, we monitored the abundance of this mRNA in the various mutant strains (Figure 1B). In contrast to *wt* cells, the induction of *ste11*$^+$ mRNA was greatly delayed or virtually abolished in *fkh2*, *fkh2 fhl1*, *fkh2 mei4*, or *fkh2 fhl1 mei4* mutant cells. In *fhl1*-deleted cells, the increase in *ste11*$^+$ mRNA was apparent, but slightly reduced. In *mei4*-deleted cells, the increase in *ste11*$^+$ mRNA was apparent but delayed. Ectopic expression of *ste11*$^+$ indeed restored fertility not only to the *fkh2*-deleted cells but also to *fkh2 fhl1*, *fkh2 mei4*, and *fkh2 fhl1 mei4* mutant cells to an extent similar to that observed with ectopic expression of *fkh2*$^+$ (Figure 1C). We thus concluded that the sterility of the forkhead mutant cells was caused largely by poor induction of *ste11*$^+$, not by slow growth. In addition, the sterility was not attributable to a defect in the induction of G_1 arrest by nitrogen starvation, given that the forkhead mutant cells arrested in G_1 phase in a manner similar to that of *wt* cells (Supplementary Figure 1).

Fkh2p binds to a FLEX element upstream of ste11$^+$ *both in vivo and in vitro*

Given that the forkhead family of transcription factors recognizes the core sequence GTAAAYA (Pierrou *et al*, 1994), we searched for this sequence in the vicinity of the genomic locus of *ste11*$^+$. One such sequence, designated FLEX1, was detected in the putative 5′ regulatory region of *ste11*$^+$ (Figure 2A). If one mismatched base is allowed, three FLEX-like sequences—designated FLEXL1, FLEXL2, and FLEXL3—were also apparent in this region.

To examine whether Fkh2p binds to these FLEX or FLEX-like elements, we prepared a fusion protein consisting of glutathione-*S*-transferase (GST) and the forkhead DNA-binding domain of Fkh2p (amino acids 216–330) and performed an electrophoretic mobility-shift assay (EMSA) with this protein and radioactive oligonucleotides containing the FLEX1 or FLEXL sequences as probes (Figure 2B). Shifted bands were observed with FLEX1 and, to a lesser extent, with FLEXL1, but they were not detected with FLEXL2, FLEXL3, or an unrelated (TR) probe. The shifted bands were specific for Fkh2p and for FLEX1 or FLEXL1, given that they were not observed with GST in place of the fusion protein and that the corresponding unlabeled oligonucleotides, but not an unrelated oligonucleotide (TR), inhibited the binding of the GST–Fkh2 fusion protein to the labeled probes. The shifted band observed with the FLEX1 probe was also supershifted in the presence of antibodies to GST. These results thus indicated that the GST–Fkh2 fusion protein directly binds to FLEX1 and, to a lesser extent, to FLEXL1 *in vitro*.

To examine whether Fkh2p binds to the FLEX or FLEX-like sequences upstream of *ste11*$^+$ *in vivo*, we performed a chromatin immunoprecipitation (ChIP) assay with cells expressing green fluorescent protein (GFP)-tagged Fkh2p by *nmt41* promoter (Figure 2C). In cells expressing GFP-tagged Fkh2p, the mating efficiency and the induction of *ste11*$^+$ mRNA were comparable to those in *wt* cells, suggesting that GFP-tagged Fkh2p functions like *wt* protein (Supplementary Figure 2). Immunoprecipitation with antibodies to GFP revealed that GFP-Fkh2p associates with genomic DNA containing both FLEX1 and FLEXL1 (primer set A), whereas association with genomic DNA containing both FLEXL2 and FLEXL3 (primer set B) is little. The amount of either region of genomic DNA immunoprecipitated with the antibodies to GFP was greatly reduced for cells not expressing GFP-Fkh2p. These results showed that Fkh2p binds *in vivo* to the genomic locus containing the FLEX1 and FLEXL1 elements upstream of *ste11*$^+$. To test whether such binding depends on nutrient conditions, we measured the binding activity of Fkh2p in cells subjected to nitrogen deprivation. The ChIP assay revealed that nitrogen withdrawal resulted in an increase in the binding of GFP-Fkh2p to genomic DNA containing FLEX1 and FLEXL1 (Figure 2D), but not to the region upstream of *cdc15*$^+$ (Supplementary Figure 3). The amount of genomic DNA containing FLEX1 and FLEXL1 immunoprecipitated with the antibodies to GFP was low for cells not expressing GFP-Fkh2p upon nitrogen starvation. These results suggest that Fkh2p associates with the upstream region of *ste11*$^+$ *in vivo* when cells are able to mate.

To examine the role of FLEX1 in mating, we deleted the 7-bp core sequence of this site from its chromosome locus. The mating efficiency of the resulting mutant strain (*ste11-dFLEX1*) was greatly reduced compared with that of *wt* cells (Figure 2E; Supplementary Figure 2). This sterility was not attributable to a defect in induction of G_1 arrest (Supplementary Figure 4). These observations suggested that the core sequence of FLEX1 is required for efficient mating. In addition, induction of *ste11*$^+$ mRNA by nitrogen withdrawal was largely abolished in *ste11-dFLEX1* cells (Figure 2F; Supplementary Figure 2), suggesting that the core sequence of FLEX1 is also required for activation of

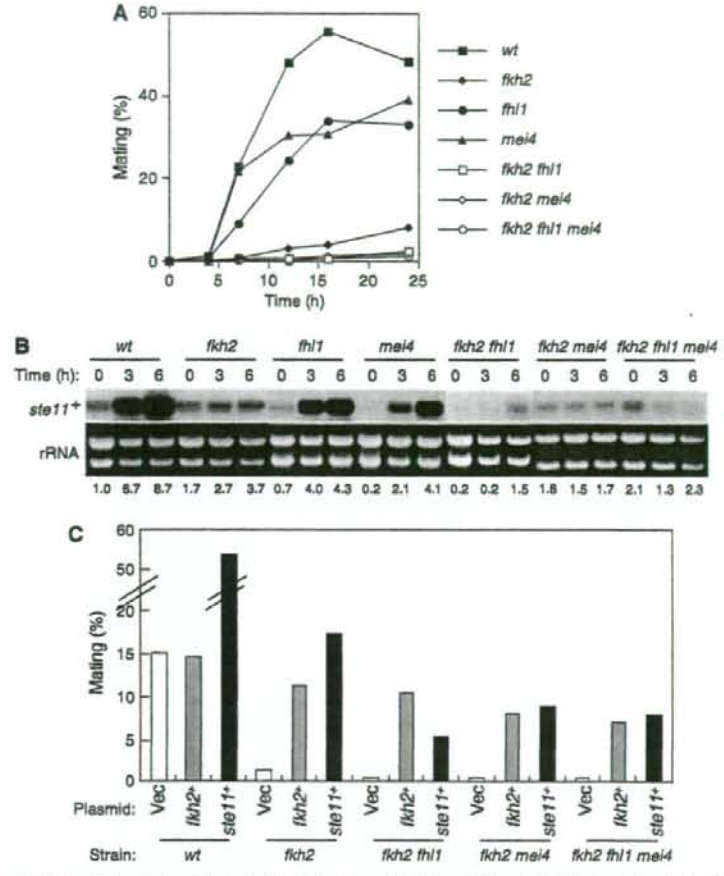

Figure 1 Forkhead transcription factors are required for the induction of *ste11*$^+$ mRNA and efficient mating. (**A**) *wt* (HM6), *fkh2* (HM5657), *fhl1* (HM4837), *mei4* (HM50), *fkh2 fhl1* (HM4887), *fkh2 mei4* (HM5515), or *fkh2 fhl1 mei4* (HM5544) cells were grown in EMM2 medium to a density of 1×10^7 cells/ml, washed, and resuspended at a density of 2×10^7 cells/ml in EMM2 medium lacking nitrogen. They were then cultured at 30°C and samples were collected at the indicated times for determination of mating frequency. Data are from representative experiments. (**B**) Total RNA was extracted from cells treated as in (A), and the abundance of *ste11*$^+$ mRNA was examined by northern blot analysis. Ethidium bromide staining of rRNA is shown as a loading control. The ratios of intensities of *ste11*$^+$ to rRNA signals were used to calculate the relative fold enrichment, shown below the rRNA. The samples from *wt* to *fkh2*, from *fhl1* to *mei4*, from *fkh2 mei4* to *fkh2 fhl1 mei4* were from the same gel. All the samples were treated equally and the exposure time was the same. (**C**) Cells were transformed with pcL-*ste11*$^+$ (*ste11*$^+$), pAL-*fkh2*$^+$ (*fkh2*$^+$), or the empty vector pcL-X (Vec) and were cultured as in (A) for the determination of mating efficiency at 24 h after transfer to EMM2 medium without nitrogen. Data are from representative experiments.

ste11$^+$ expression. The ChIP assay revealed that the core FLEX deletion resulted in a decrease in the binding of GFP-Fkh2p to genomic DNA around FLEX1 (Figure 2D), suggesting that the core FLEX1 is required for Fkh2p to associate with the upstream region of *ste11*$^+$ *in vivo*.

Effects of phosphorylation of Fkh2p by Cdc2p

Cdks regulate forkhead transcription factors in various organisms, and Fkh2p has been shown to be a phosphoprotein in fission yeast (Buck *et al*, 2004; Bulmer *et al*, 2004). A search of the Fkh2p sequence for consensus phosphorylation sites for Cdc2p, (pS/pT)-P-X-(R/K) (Nigg, 1993), revealed three such sites at residues T314, S462, and S481 (Figure 3A). The sequence surrounding T314 in the DNA-binding domain of Fkh2p is conserved among members of the forkhead-box family of other species, especially those of the FoxN subfamily (Mazet *et al*, 2003), although the consensus phosphorylation site sequence is not fully conserved. S462 is conserved, but not as a Cdc2p phosphorylation site, among members of the FoxJ subfamily of transcription factors (Mazet *et al*, 2003). To assess the potential function of these putative Cdc2p phosphorylation sites in Fkh2p, we changed the serine or threonine residues to glutamic acid by site-directed mutagenesis of the chromosome to mimic the effect of Cdc2p phosphorylation *in vivo*. Cells in which T314 (*fkh2-T314E*) or S462 (*fkh2-S462E*) of Fkh2p was replaced with glutamic acid exhibited a reduced mating efficiency (Figure 3B). In contrast, similar mutation of S481 of Fkh2p (*fkh2-S481E*) did not substantially affect mating efficiency (data not shown). In addition, the mating efficiency

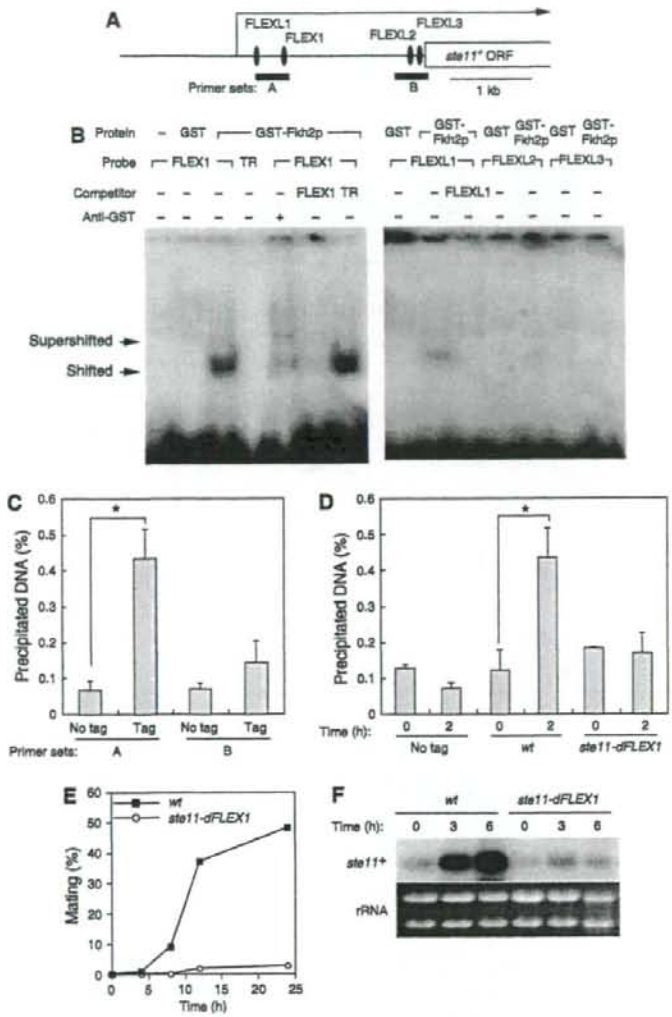

Figure 2 Fkh2 binds to FLEX and FLEXL sequences in the putative promoter region of *ste11*$^+$ and thereby induces *ste11*$^+$ mRNA. (**A**) Schematic representation of the region upstream of the open reading frame (ORF) of *ste11*$^+$ showing FLEX and FLEXL sequences. The major transcription initiation site of *ste11*$^+$ is indicated by the arrow, and the regions targeted by primer sets in ChIP analysis are also shown. (**B**) An EMSA was performed with recombinant GST–Fkh2p(216–330) (or GST alone) and with FLEX1, FLEXL1, FLEXL2, FLEXL3, or TR (negative control) probes labeled with ^{32}P. Competition was evaluated with excess amounts of unlabeled FLEX1, TR, or FLEXL1 oligonucleotides, and supershift analysis was performed with antibodies to GST, as indicated. The positions of shifted and supershifted bands are shown. (**C**) No tagged cells (no tag, HM6) and cells expressing GFP-tagged Fkh2p (Tag, HM5719) were grown to late log-phase, washed, and resuspended in medium without nitrogen. After incubation for 2 h at 30°C, cells were collected and analyzed by ChIP with antibodies to GFP and with the primer sets indicated in (A). Data are means ± s.e. $^*P<0.006$ (Student's *t*-test). (**D**) No tagged cells (no tag, HM6) and cells expressing GFP-tagged Fkh2p (*wt*; HM5719 and *ste11-dFLEX1*: HM6124) were treated and analyzed as in (C) with primer set A. Samples were collected at 0 and 2 h after nitrogen withdrawal. Data are means ± s.e. of values from three separate experiments. $^*P<0.007$ (Student's *t*-test). (**E**) *wt* (HM6) or *ste11-dFLEX1* (HM5832) cells were treated and analyzed for mating efficiency as in Figure 1A. (**F**) Total RNA was extracted from cells treated as in (E) and was subjected to northern blot analysis of *ste11*$^+$ mRNA.

of *fkh2-T314E S462E S481E* mutant cells was similar to that of *fkh2-T314E* or *fkh2-S462E* cells (Figure 3B). These results suggested that dephosphorylation of Fkh2p at T314 and S462 is required for efficient mating. However, unphosphorylated form of Fkh2p (*fkh2-T314A S462A S481A*) failed to enhance mating efficiency, suggesting that an additional mechanism is required for ectopic mating (Figure 3B). The induction of *ste11*$^+$ mRNA in response to nitrogen deprivation was greatly reduced in *fkh2-T314E* or *fkh2-S462E* cells compared with that apparent in *wt* cells (Figure 3C). These observations thus suggested that dephosphorylation of Fkh2p on T314 and S462 is required for efficient induction of *ste11*$^+$ mRNA.

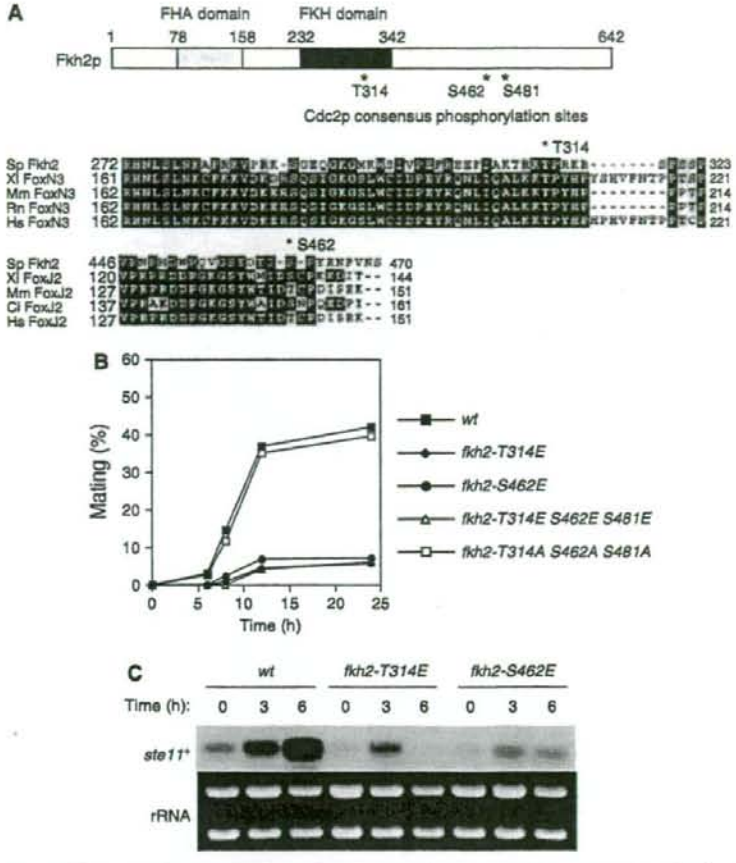

Figure 3 Phosphorylation of Fkh2p by Cdc2p negatively regulates mating. (**A**) A schematic representation of Fkh2p indicating consensus phosphorylation sites (T314, S462, S481) for Cdc2p as well as the FHA and FKH domains is shown in the upper panel. Multiple alignment of Fkh2, FoxN3, and FoxJ2 proteins of *S. pombe* (Sp), *Xenopus laevis* (Xl), *Mus musculus* (Mm), *Rattus norvegicus* (Rn), *Homo sapiens* (Hs), and *Ciona intestinalis* (Cl) is shown in the lower panels. Identical (shaded black) and similar (shaded gray) amino acids as well as two Cdc2p consensus phosphorylation sites (T314 and S462) of Fkh2p are indicated. Dashes represent gaps introduced to optimize alignment. (**B**) Cells expressing wild type (*wt*, HM5145) or T314E (*fkh2-T314E*, HM5910), S462E (*fkh2-S462E*, HM5911), T314E S462E S481E (*fkh2-T314E S462E S481E*, HM5827) or T314A S462A S481A (*fkh2-T314A S462A S481A*, HM5722) mutant forms of Fkh2p were treated and analyzed for mating efficiency as in Figure 1A. (**C**) Total RNA was extracted from cells treated as in (B) and was subjected to northern blot analysis of *ste11*$^+$ mRNA.

Other defects of *fkh2*-deleted cells, such as abnormal morphology or septation defect, were less than 1% in *wt*, *fkh2-T314E*, or *fkh2-S462E* cells. In addition, cell length is similar in *wt*, *fkh2-T314E*, or *fkh2-S462E* cells (Supplementary Figure 5). These facts suggest that these point mutations specifically affect mating. To confirm that these point mutations do not affect cell-cycle progression and transcriptional activity during the normal mitotic cell cycle, we measured the timing of mitotic entry and the mRNA levels of *cdc15*$^+$, *spo12*$^+$, and *slp1*$^+$, as Fkh2p is required for periodic expression of these mRNAs (Buck *et al*, 2004; Bulmer *et al*, 2004). Cells were transiently arrested in late G_2 by the inactivation of *cdc25*$^+$ and released to the permissive temperature to enter a synchronous cell cycle. In contrast to *fkh2*-deleted cells that showed the severe delay in entry into mitosis (Buck *et al*, 2004), *wt*, *fkh2-T314E*, or *fkh2-S462E* cells entered mitosis almost with the same timing as indicated by the coincidence of the peak of septa (Supplementary Figure 6). Additionally, the periodic expressions of *cdc15*$^+$, *spo12*$^+$, and *slp1*$^+$ mRNAs were observed in *wt*, *fkh2-T314E*, or *fkh2-S462E* cells (Supplementary Figure 6). These results suggest that these point mutations specifically affect *ste11*$^+$ mRNA expression but not other mitotic genes expression. The poor mating efficiency of the *fkh2-T314E* or *fkh2-S462E* mutants was not due to a defect in induction of cell-cycle arrest in G_1 phase (Supplementary Figure 7). In addition, the abundance of the mutant proteins was similar to that of the wild-type protein (Supplementary Figure 8), suggesting that the poor mating efficiency of the mutant cells was not attributable to a reduced protein level.

Phosphorylation of Fkh2p by Cdc2p in vitro and in vivo

We next tested whether Cdc2p directly phosphorylates GST fusion proteins containing various fragments of Fkh2p

